

Differentially-Private Hierarchical Federated Learning

Frank Po-Chen Lin and Christopher Brinton
Electrical and Computer Engineering, Purdue University
{lin1183,cgb}@purdue.edu

ABSTRACT

While federated learning (FL) eliminates the transmission of raw data over a network, it is still vulnerable to privacy breaches from the communicated model parameters. In this work, we propose Hierarchical Federated Learning with Hierarchical Differential Privacy (H^2FDP), a DP-enhanced FL methodology for jointly optimizing privacy and performance in hierarchical networks. Building upon recent proposals for Hierarchical Differential Privacy (HDP), one of the key concepts of H^2FDP is adapting DP noise injection at different layers of an established FL hierarchy – edge devices, edge servers, and cloud servers – according to the trust models within particular subnetworks. We conduct a comprehensive analysis of the convergence behavior of H^2FDP , revealing conditions on parameter tuning under which the training process converges sublinearly to a finite stationarity gap that depends on the network hierarchy, trust model, and target privacy level. Leveraging these relationships, we develop an adaptive control algorithm for H^2FDP that tunes properties of local model training to minimize communication energy, latency, and the stationarity gap while striving to maintain a sub-linear convergence rate and meet desired privacy criteria. Subsequent numerical evaluations demonstrate that H^2FDP obtains substantial improvements in these metrics over baselines for different privacy budgets, and validate the impact of different system configurations.

KEYWORDS

Federated Learning, Edge Intelligence, Differential Privacy, Hierarchical Networks

ACM Reference Format:

Frank Po-Chen Lin and Christopher Brinton. 2018. Differentially-Private Hierarchical Federated Learning. In *Proceedings of The ACM International Symposium on Mobile Ad Hoc Networking and Computing, (MobiHoc)*. ACM, New York, NY, USA, 26 pages. <https://doi.org/XXXXXXXX.XXXXXX>

1 INTRODUCTION

The concept of privacy has significantly evolved in the digital age, particularly with regards to data collection, sharing, and utilization in machine learning (ML) [2, 5]. The ability to extract knowledge from massive datasets is a double-edged sword; while empowering ML algorithms, it simultaneously exposes individuals' sensitive information. Therefore, it is crucial to develop ML methods that respect user privacy and conform to data protection standards [4, 7].

Permission to make digital or hard copies of all or part of this work for personal or classroom use is granted without fee provided that copies are not made or distributed for profit or commercial advantage and that copies bear this notice and the full citation on the first page. Copyrights for components of this work owned by others than the author(s) must be honored. Abstracting with credit is permitted. To copy otherwise, or republish, to post on servers or to redistribute to lists, requires prior specific permission and/or a fee. Request permissions from permissions@acm.org.

MobiHoc, Oct. 14–17, 2024, Athens, Greece

© 2018 Copyright held by the owner/author(s). Publication rights licensed to ACM.

ACM ISBN 978-x-xxxx-xxxx-x/YY/MM

<https://doi.org/XXXXXXXX.XXXXXX>

To this end, federated learning (FL) has emerged as an attractive paradigm for distributing ML over networks, as it allows for model updates to occur directly on the edge devices where the data originates [8, 11, 14, 25]. Information transmitted over the network is in the form of locally trained models for periodic aggregations at a central server. Nonetheless, FL is also susceptible to privacy threats: it has been shown that adversaries with access to model updates can reverse engineer attributes of device-side data [26, 28, 34]. This has motivated different threads of investigation on privacy preservation within the FL framework. One common approach has been the introduction of differential privacy (DP) mechanisms into FL [3, 12, 19–21, 24, 27, 31, 32]. DP injects calibrated noise into the data or query responses to prevent the leakage of individual-level information, creating a privacy-utility tradeoff for FL.

In this work, we are interested in examining and improving the privacy-utility tradeoff for DP infusion over practical FL deployments. We focus particularly on *hierarchical* FL (HFL) systems, where a layer of fog network elements (e.g., edge servers) separate edge devices from the cloud server, and conduct intermediate model aggregations [3, 9, 11]. These intermediate nodes offer additional flexibility into where and how DP noise injection occurs, but challenge our understanding of how DP impacts performance metrics in HFL, and how the tradeoffs can be controlled systematically. Motivated by this, we investigate the following questions:

- (1) *What is the coupled effect between HFL system configuration and DP noise injection on model training performance?*
- (2) *How can we adapt DP and HFL to jointly optimize ML performance, privacy preservation, and resource utilization?*

1.1 Related Work

The introduction of DP into FL has traditionally followed two paradigms: (i) central DP (CDP), involving noise addition at the main server [10, 29], and (ii) local DP (LDP), which adds noise at each edge device [12, 17, 19, 32]. CDP generally leads to a more accurate final model, but it hinges on the trustworthiness of the main server. Conversely, LDP forgoes this trust requirement but requires a higher level of noise addition at each device to compensate [16].

There have been several research efforts dedicated to integrating these two paradigms into HFL, e.g., [3, 20, 23, 33]. [20, 33] adapted the LDP strategy to the hierarchical FL structure, utilizing moment accounting to obtain strict privacy guarantees across the system. [23] explored the advantages of flexible decentralized control over the training process in hierarchical FL and examined its implications on participant privacy. More recently, a third paradigm called hierarchical DP (HDP) has been introduced [3]. HDP assumes that certain “super-nodes” present within the network (e.g., edge/fog servers, intermediate routers) can be trusted even if the main server cannot. These super-nodes are entrusted with the task of adding calibrated DP noise to the aggregated models prior to transmission. Instead of injecting noise uniformly, HDP enables tailoring noise

addition to varying levels of trust within the system, highlighting an opportunity for privacy amplification at the “super-node” level.

Despite these efforts, *none have yet attempted to rigorously characterize or optimize a system that fuses the flexible trust model of HDP with HFL training procedures.* In this work, we bridge this gap through the development of *Hierarchical Federated Learning with Hierarchical Differential Privacy* (H²FDP), along with its associated theoretical analysis and a control algorithm. Our convergence analysis reveals conditions necessary to secure robust convergence rates in DP-enhanced HFL systems, providing a foundation for our control algorithm designed to adapt the tradeoff among energy consumption, training delay, model accuracy, and data privacy.

1.2 Outline and Summary of Contributions

- We formalize H²FDP, which integrates flexible HDP trust models with hierarchical FL (Sec. 3). H²FDP is designed to preserve a target privacy level throughout the entire training process, instead of only at individual aggregations, allowing for a more effective balance between privacy preservation and model performance.
- We theoretically characterize the convergence behavior of H²FDP under non-convex ML loss functions (Sec. 4). Our analysis (culminating in Theorem 4.3) shows that with an appropriate choice of FL step size, the cumulative average global model will converge sublinearly with rate $\mathcal{O}(1/\sqrt{k})$ to a region around a stationary point. The stationarity gap depends on factors including the trust model, network layout, and aggregation intervals.
- Leveraging our convergence results, we develop an adaptive control algorithm for H²FDP (Sec. 5). This algorithm simultaneously optimizes communication energy, latency, and model training performance, while maintaining the sub-linear convergence rate and desired privacy standards. This is achieved through fine-tuning the local training interval length, learning rate, and fraction of devices engaged in FL in each edge cluster.
- Through numerical evaluations, we demonstrate that H²FDP obtains substantial improvements in convergence speed and trained model accuracy relative to existing DP-based FL algorithms (Sec. 6). Further, we find that the control algorithm reduce energy consumption and delay by up to 60%. Our results also corroborate the impact of the network configuration and trust model on training performance in our bounds.

All proofs of results have been deferred to Appendices A-C.

2 PRELIMINARIES AND SYSTEM MODEL

This section introduces key DP concepts (Sec. 2.1), our hierarchical network model (Sec. 2.2), and the target ML task (Sec. 2.3).

2.1 Differential Privacy (DP)

Differential privacy (DP) characterizes a randomization technique according to parameters ϵ, δ . Formally, a randomized mechanism \mathcal{M} adheres to (ϵ, δ) -DP if it satisfies the following:

Definition 2.1 ((ϵ, δ) -DP [6]). For all datasets \mathcal{D} and \mathcal{D}' differing in at most one element, and for all $\mathcal{S} \subseteq \text{Range}(\mathcal{M})$, it holds that:

$$\Pr[\mathcal{M}(\mathcal{D}) \in \mathcal{S}] \leq e^\epsilon \Pr[\mathcal{M}(\mathcal{D}') \in \mathcal{S}] + \delta, \quad (1)$$

where $\epsilon > 0$ and $\delta \in (0, 1)$.

ϵ represents the privacy budget, quantifying the degree of uncertainty introduced in the privacy mechanism. Smaller ϵ implies a stronger privacy guarantee. δ bounds the probability of the privacy mechanism being unable to preserve the ϵ -privacy guarantee.

Gaussian Mechanism: The Gaussian mechanism is a commonly employed randomization mechanism compatible with (ϵ, δ) -DP. With it, noise sampled from a Gaussian distribution is introduced to the output of the function being applied to the dataset. This function, in the case of H²FDP, is the computation of gradients.

Formally, to maintain (ϵ, δ) -DP for any query function f processed utilizing the Gaussian mechanism, we must have

$$\Delta^2 f \leq \frac{2 \log(1.25/\delta)}{\epsilon^2}, \quad (2)$$

where Δf is the L_2 -sensitivity, and ϵ, δ are the privacy parameters.

L_2 -Sensitivity: The sensitivity of a function is a measure of how much the output can change due to the modification of a single record in the input dataset. Specifically, the L_2 -sensitivity for a function f is defined as:

$$\Delta f = \max_{\mathcal{D}, \mathcal{D}'} \|f(\mathcal{D}) - f(\mathcal{D}')\|_2, \quad (3)$$

where $\|\cdot\|_2$ is the L_2 norm. In our setting, L_2 sensitivity allows calibrating the amount of Gaussian noise to be added to ensure the desired (ϵ, δ) -differential privacy in FL model training.

2.2 Hierarchical Network System Model

System Architecture: We consider the hierarchical network architecture depicted in Fig. 1. The hierarchy, from bottom to top, consists of local edge devices $\mathcal{I} = \{1, \dots, I\}$, edge servers $\mathcal{N} = \{n_1, \dots, n_N\}$, and the cloud server. The primary responsibilities of these layers include local model training (edge devices), local aggregation (edge servers), and global aggregation (cloud server).

The edge devices are organized into N subnets (or clusters) $\{\mathcal{S}_c\}_{c=1}^N$, each of which is linked to a specific edge server for up/down-link model transmissions. Each edge server $n_c \in \mathcal{N}$ is associated with a distinct subnet \mathcal{S}_c . The size of each subnet \mathcal{S}_c is denoted by $s_c = |\mathcal{S}_c|$, where the total number of devices is $I = \sum_{c=1}^N s_c$.

Threat Model: We further categorize the set of edge servers \mathcal{N} into (i) *secure/trusted* edge servers, $\mathcal{N}_T \subseteq \mathcal{N}$, and (ii) *insecure/untrusted* edge servers, $\mathcal{N}_U \subseteq \mathcal{N}$. We make no particular assumptions on how this designation is made; for instance, a network operator may provide service through a combination of its own infrastructure (trusted/secure) as well as borrowed infrastructure (untrusted/insecure). With the exception of the trusted edge servers, i.e., $n_c \in \mathcal{N}_T$, all participating entities – namely, the edge devices, i.e., $i \in \mathcal{I}$, the untrusted edge servers, i.e., $n_c \in \mathcal{N}_U$, and the cloud server – are presumed to exhibit *semi-honest behavior* [15, 26, 34]. In particular, despite adhering to the hierarchical FL protocol, we assume there is a possibility that these semi-honest entities may seek to extract sensitive information from shared FL models.

2.3 Machine Learning Model

Each edge device $i \in \mathcal{I}$ has a dataset \mathcal{D}_i comprised of $D_i = |\mathcal{D}_i|$ data points. We consider the datasets \mathcal{D}_i to be non-i.i.d. across devices, as is standard in FL research.

The loss $\ell(d; \mathbf{w})$ quantifies the fit of the ML model to the learning task. It is linked to a data point $d \in \mathcal{D}_i$ and depends on the ML

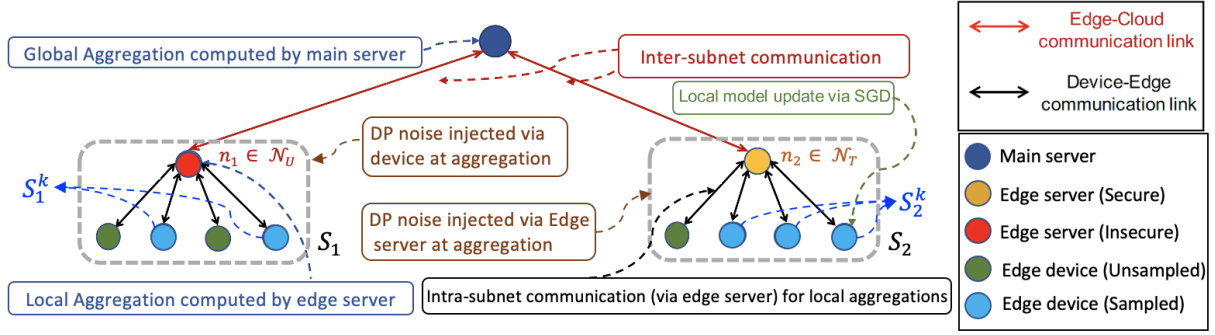


FIGURE 1: **Two-layer network architecture showing two local subnets, S_1 and S_2 . Insecure edge server $n_1 \in \mathcal{N}_U$ serves devices $j \in S_1$, with a subset S_1^k participating in the k -th local training interval. Secure edge server $n_2 \in \mathcal{N}_T$ serves devices $j \in S_2$.**

model parameter vector $\mathbf{w} \in \mathbb{R}^M$ (with M representing the model's dimension). Consequently, the *local loss function* for device i is:

$$F_i(\mathbf{w}) = \frac{1}{D_i} \sum_{(x,y) \in \mathcal{D}_i} \ell(\mathbf{x}, y; \mathbf{w}). \quad (4)$$

We further define the *subnet-level loss function* for each S_c as

$$\bar{F}_c(\mathbf{w}) = \sum_{i \in S_c} \rho_{i,c} F_i(\mathbf{w}), \quad (5)$$

where $\rho_{i,c} = 1/s_c$ symbolizes the relative weight of edge device $i \in S_c$ within its subnet. Finally, the *global loss function* is defined as the average loss across all subnets:

$$F(\mathbf{w}) = \sum_{c=1}^N \varrho_c \bar{F}_c(\mathbf{w}), \quad (6)$$

where $\varrho_c = 1/N$ is each subnet's contribution to the global loss.

The primary objective of ML model training is to pinpoint the optimal global model parameter vector $\mathbf{w}^* \in \mathbb{R}^M$ such that $\mathbf{w}^* = \arg \min_{\mathbf{w} \in \mathbb{R}^M} F(\mathbf{w})$.

3 PROPOSED METHODOLOGY

In this section, we formalize H²FDP, including its operation timescales (Sec. 3.1), training process (Sec. 3.2), and DP mechanism (Sec. 3.3).

3.1 Model Training Timescales

Training in H²FDP follows a slotted-time representation, depicted in Fig. 2. *Local model training iterations* are carried out by edge devices via stochastic gradient descent (SGD) at each time index $t = 0, 1, \dots, T$. The duration from 0 to T is divided into K_g *local model training intervals*, denoted by $k = 0, 1, \dots, K_g - 1$. Each interval, $\mathcal{T}_k = \{t_k + 1, \dots, t_{k+1}\} \subset \{0, 1, \dots, T\}$, is of length $\tau_k = |\mathcal{T}_k|$.

We also consider that only a fraction of devices in each subnet may be active in each local interval, as depicted in Fig. 1. Formally, we define $S_c^k \subseteq S_c$ as the subset of devices in subnet c engaged in iteration k , with size denoted $s_c^k = |S_c^k|$. The parameters τ_k, s_c^k will be treated as parameters in our control algorithm in Sec. 5 to balance between learning, resource, and privacy metrics.

H²FDP begins with the cloud server broadcasting the initial global model $\bar{\mathbf{w}}^{(0)}$ to all devices at $t_0 = 0$. Local training interval k is book-ended by *global aggregations* at times t_k and t_{k+1} . For $t \in \mathcal{T}_k$, each edge device applies SGD iterations on its local dataset. Edge server c performs intermittent *local aggregations* at times $t \in \mathcal{T}_{k,c}^L$, where

$\mathcal{T}_{k,c}^L \subset \mathcal{T}_k$ is the set of local aggregation instances for subnet c in interval k , and $K_{k,c} = |\mathcal{T}_{k,c}^L|$. We formalize these steps next.

3.2 H²FDP Training and Aggregations

Local model update: At time $t \in \mathcal{T}_k$, device i randomly selects a mini-batch $\xi_i^{(t)}$ from its local dataset \mathcal{D}_i . Using this mini-batch, it calculates the unbiased *stochastic gradient estimate* based on its preceding local model $\mathbf{w}_i^{(t)}$:

$$\hat{\mathbf{g}}_i^{(t)} = \frac{1}{|\xi_i^{(t)}|} \sum_{(x,y) \in \xi_i^{(t)}} \nabla \ell(\mathbf{x}, y; \mathbf{w}_i^{(t)}). \quad (7)$$

We assume a uniform selection probability q of each data point, i.e., $q = |\xi_i^{(t)}|/D_i, \forall i$. Device i employs $\hat{\mathbf{g}}_i^{(t-1)}$ to determine its *provisional updated local model* $\tilde{\mathbf{w}}_i^{(t)}$:

$$\tilde{\mathbf{w}}_i^{(t)} = \mathbf{w}_i^{(t-1)} - \eta_k \hat{\mathbf{g}}_i^{(t-1)}, \quad t \in \mathcal{T}_k, \quad (8)$$

Here, $\eta_k > 0$ signifies the step size. Using $\tilde{\mathbf{w}}_i^{(t)}$ as the base, the *final updated local model* $\mathbf{w}_i^{(t)}$ is determined in one of several ways depending on the trust model, described next.

If a subnet S_c does not perform a local aggregation at a specific time t , i.e., $t \in \mathcal{T}_k \setminus \mathcal{T}_{k,c}^L$, the updated model follows $\mathbf{w}_i^{(t)} = \tilde{\mathbf{w}}_i^{(t)}$ in (8). On the other hand, if $t \in \mathcal{T}_{k,c}^L$, then the updated local model inherits the local model aggregation described next.

Local model aggregations: When $t \in \mathcal{T}_{k,c}^L$, there are two possibilities depending on the subnet trust model:

(i) *Subnets with secure edge servers:* If the edge server for subnet S_c is considered trustworthy, i.e., $n_c \in \mathcal{N}_T$, each device i in the subnet sends the server its accumulated local stochastic gradient $\eta_k \sum_{\ell=t'}^t \hat{\mathbf{g}}_i^{(\ell)}$ since the last local aggregation, with no additional noise attached. The edge server computes the *local aggregated model* $\bar{\mathbf{w}}_c^{(t)}$ by determining the weighted average of the aggregated gradients across all edge devices within the same subnet, followed by integrating DP noise $\bar{\mathbf{n}}_{c,Loc}^{(t)} \sim \mathcal{N}(0, \sigma_{c,Loc}^2 \mathbf{I}_M), \forall c$. The edge server adjusts the prior local aggregated model $\bar{\mathbf{w}}_c^{(t')}$ as follows:

$$\bar{\mathbf{w}}_c^{(t)} = \bar{\mathbf{w}}_c^{(t')} - \eta_k \sum_{\ell=t'}^t \sum_{j \in S_c} \rho_{j,c} \hat{\mathbf{g}}_j^{(\ell)} + \bar{\mathbf{n}}_{c,Loc}^{(t)}, \quad (9)$$

where $t' \in \mathcal{T}_{k,c}^L$ is the time index of the previous aggregation.

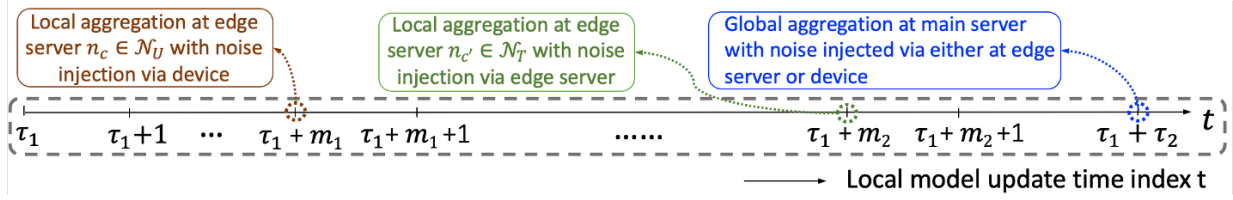


FIGURE 2: **Illustration of timescales in H^2FDP .** In this example, $t = \tau_1 + m_1$ marks local aggregation in subnet S_c linked to insecure edge server $n_c \in \mathcal{N}_U$, while $t = \tau_1 + m_2$ denotes local aggregation in subnet $S_{c'}$ connected to secure edge server $n_{c'} \in \mathcal{N}_T$.

(ii) *Subnets with insecure edge servers:* Conversely, if edge server n_c is considered untrustworthy, i.e., $n_c \in \mathcal{N}_U$, device i within subnet S_c injects DP noise $\mathbf{n}_{i,Loc}^{(t)} \sim \mathcal{N}(0, \sigma_{i,Loc}^2 \mathbf{I}_M)$ within its transmission. Upon receipt of the noisy accumulated gradients, the server computes the $\bar{\mathbf{w}}_c^{(t)}$ as the weighted average of the noisy summed gradients across edge devices in the same subnet. This leads to the following adjustment from the previous aggregated model $\bar{\mathbf{w}}_c^{(t')}$:

$$\bar{\mathbf{w}}_c^{(t)} = \bar{\mathbf{w}}_c^{(t')} - \eta_k \sum_{t'=t'}^t \sum_{j \in S_c} \rho_{j,c} \widehat{\mathbf{g}}_j^{(t')} + \sum_{j \in S_c} \rho_{j,c} \mathbf{n}_{j,Loc}^{(t)}. \quad (10)$$

Combining (9)&(10), we can express

$$\bar{\mathbf{w}}_c^{(t)} = \sum_{i \in S_c} \rho_{i,c} \tilde{\mathbf{w}}_i^{(t)} + \bar{\mathbf{n}}_{c,Loc}^{(t)}, \quad (11)$$

where

$$\bar{\mathbf{n}}_{c,Loc}^{(t)} = \begin{cases} \tilde{\mathbf{n}}_{c,Loc}^{(t)}, & n_c \in \mathcal{N}_T, \\ \sum_{j \in S_c} \rho_{j,c} \mathbf{n}_{j,Loc}^{(t)}, & n_c \in \mathcal{N}_U. \end{cases} \quad (12)$$

Finally, after computing the local aggregated model, the edge server n_c broadcasts $\bar{\mathbf{w}}_c^{(t)}$ across its subnet. The devices subsequently synchronize their local models as $\mathbf{w}_i^{(t)} = \bar{\mathbf{w}}_c^{(t)}$, $i \in S_c$.

Based on this, the local model update process for each device $i \in S_c$ at time t can be summarized as

$$\mathbf{w}_i^{(t)} = (1 - \Theta_c^{(t)}) \tilde{\mathbf{w}}_i^{(t)} + \Theta_c^{(t)} \bar{\mathbf{w}}_c^{(t)}, \quad \forall t \in \mathcal{T}_k, \quad (13)$$

where $\Theta_c^{(t)} = 1$ if $t \in \mathcal{T}_{k,c}^L$, and $\Theta_c^{(t)} = 0$ otherwise.

Global model aggregation: At the end of each local model training interval \mathcal{T}_k , i.e., at $t = t_{k+1}$, a global aggregation occurs. Once again, devices handle this process differently according to their subnet's security model:

(i) *Subnets with secure edge servers:* Devices within trusted subnets transmit their accumulated local stochastic gradients since the last global aggregation without the addition of extra noise. Edge servers calculate the weighted average of these aggregated gradients across all devices within their subnets. Following this, they incorporate a differentially private noise $\bar{\mathbf{n}}_{c,Glob}^{(t)} \sim \mathcal{N}(0, \bar{\sigma}_{c,Glob}^2 \mathbf{I}_M)$, $\forall c$, and upload the result to the main server.

(ii) *Subnets with insecure edge servers:* In the case of untrusted subnets, each device sends out its cumulative local stochastic gradients from the last local aggregation, but with an added DP noise $\mathbf{n}_{i,Glob}^{(t)} \sim \mathcal{N}(0, \sigma_{i,Glob}^2 \mathbf{I}_M)$, $\forall i$. Upon reception, the edge servers determine the weighted average of these gradients across devices within the same subnet and relay this to the main server.

Subsequently, the main server updates the global model. After computing the weighted average of the noisy accumulated gradients, the expression for the update of the previous $\bar{\mathbf{w}}^{(t_k)}$ is:

$$\begin{aligned} \bar{\mathbf{w}}^{(t)} &= \bar{\mathbf{w}}^{(t_k)} - \eta_k \sum_{t=t_k}^{t_{k+1}} \sum_{c=1}^N \varrho_c \sum_{j \in S_c} \rho_{j,c} \widehat{\mathbf{g}}_j^{(t)} \\ &+ \sum_{t \in \mathcal{T}_{k,c}^L} \sum_{c=1}^N \varrho_c \bar{\mathbf{n}}_{c,Loc}^{(t)} + \bar{\mathbf{n}}_{Glob}^{(t_{k+1})}, \end{aligned} \quad (14)$$

Upon completion of the calculations at the main server, the resulting global model $\bar{\mathbf{w}}^{(t_{k+1})}$ is employed to synchronize the local models maintained by the edge devices, i.e., $\mathbf{w}_i^{(t)} = \bar{\mathbf{w}}^{(t)} \forall i$.

3.3 DP Mechanisms

We now dictate the procedure for configuring the DP noise variables $\tilde{\mathbf{n}}_{c,Loc}^{(t)}$ and $\bar{\mathbf{n}}_{c,Glob}^{(t)}$ introduced by the edge server, along with $\mathbf{n}_{i,Loc}^{(t)}$ and $\mathbf{n}_{i,Glob}^{(t)}$ incorporated by the edge devices. In this study, we focus on the Gaussian mechanisms from Sec. 2.1, though H^2FDP can be adjusted to accommodate other DP mechanisms too.

Following the composition rule of DP [6], we aim to take into account the privacy budget *across all aggregations throughout the training*. This will ensure cumulative privacy for the complete model training process, rather than considering each individual aggregation in isolation [19, 27]. Below, we define the Gaussian mechanisms, incorporating the moment accountant technique [20, 33]. These mechanisms utilize (20) from Assumption 2 which is stated in Sec. 4.

PROPOSITION 3.1 (GAUSSIAN MECHANISM [1]). *Under Assumption 2, there exists constants c_1 and c_2 such that given the data sampling probability q at each device, and the total number of aggregations L conducted during the model training process, for any $\epsilon < c_1 qL$, H^2FDP exhibits (ϵ, δ) -differential privacy for any $\delta > 0$, so long as the DP noise follows $\mathbf{n}_{DP}^{(t)} \sim \mathcal{N}(0, \sigma_{DP}^2 \mathbf{I}_M)$, where*

$$\sigma_{DP} = c_2 \frac{q \Delta \sqrt{L \log(1/\delta)}}{\epsilon}. \quad (15)$$

Here, Δ represent the L_2 -norm sensitivity of the gradients exchanged during the aggregations.

The characteristics of the DP noises introduced during local and global aggregations can be established using Proposition 3.1. The relevant L_2 -norm sensitivities can be established as follows:

LEMMA 3.2. *Under Assumption 2, the L_2 -norm sensitivity of the exchanged gradients during local aggregations can be obtained as:*

$$\begin{aligned}\bar{\Delta}_{c,Loc} &= \max_{\mathcal{D}, \mathcal{D}'} \left\| \eta_k \sum_{t=t'}^t \sum_{j \in \mathcal{S}_c} \rho_{j,c} \left(\widehat{\mathbf{g}}_j^{(t)}(\mathcal{D}) - \widehat{\mathbf{g}}_j^{(t)}(\mathcal{D}') \right) \right\| \\ &= 2\eta_k \tau_k G / s_c,\end{aligned}\quad (16)$$

$$\Delta_{i,Loc} = \max_{\mathcal{D}, \mathcal{D}'} \left\| \eta_k \sum_{t=t'}^t \widehat{\mathbf{g}}_i^{(t)}(\mathcal{D}) - \eta_k \sum_{t=t'}^t \widehat{\mathbf{g}}_i^{(t)}(\mathcal{D}') \right\| = 2\eta_k \tau_k G. \quad (17)$$

Similarly, the L_2 -norm sensitivity of the exchanged gradients during global aggregations can be obtained as follows:

$$\begin{aligned}\bar{\Delta}_{c,Glob} &= \max_{\mathcal{D}, \mathcal{D}'} \left\| \eta_k \sum_{t=t_k}^{t_{k+1}} \sum_{j \in \mathcal{S}_c} \rho_{j,c} \left(\widehat{\mathbf{g}}_j^{(t)}(\mathcal{D}) - \widehat{\mathbf{g}}_j^{(t)}(\mathcal{D}') \right) \right\| \\ &= 2\eta_k \tau_k G / s_c,\end{aligned}\quad (18)$$

$$\Delta_{i,Glob} = \max_{\mathcal{D}, \mathcal{D}'} \left\| \eta_k \sum_{t=t_k}^{t_{k+1}} \widehat{\mathbf{g}}_i^{(t)}(\mathcal{D}) - \eta_k \sum_{t=t_k}^{t_{k+1}} \widehat{\mathbf{g}}_i^{(t)}(\mathcal{D}') \right\| = 2\eta_k \tau_k G. \quad (19)$$

Then, in subnets with secure edge servers, $\bar{\sigma}_{c,Loc}$ can be determined based on Proposition 3.1 and Lemma 3.2 by setting $L = \ell_c$ and $\Delta = \bar{\Delta}_{c,Loc}$, where $\ell_c = \sum_{k=0}^{K-1} K_{k,c}$ represents the total local aggregations. Similarly, $\bar{\sigma}_{c,Glob}$ can be determined by setting $L = K_g$ and $\Delta = \bar{\Delta}_{c,Glob}$. Conversely, in subnets with insecure edge servers, $\sigma_{i,Loc}$ can be determined by setting $L = \ell_c$ and $\Delta_{DP} = \Delta_{i,Loc}$. Likewise, $\sigma_{i,Glob}$ can be calculated by setting $L = K_g$ and $\Delta = \Delta_{i,Glob}$.

The full pseudocode for H²FDP can be found in App. F. In Sec. 5, we will introduce adaptive control into H²FDP, using the convergence results from the next section.

4 CONVERGENCE ANALYSIS

4.1 Analysis Assumptions

We first establish a few general and commonly employed assumptions that we will consider throughout our analysis.

ASSUMPTION 1 (CHARACTERISTICS OF NOISE IN SGD [11, 18, 19, 30]). Consider $\mathbf{n}_i^{(t)} = \widehat{\mathbf{g}}_i^{(t)} - \nabla F_i(\mathbf{w}_i^{(t)})$ as the noise of the gradient estimate through the SGD process for device i at time t . The noise variance is upper bounded by $\sigma^2 > 0$, i.e., $\mathbb{E}_t[\|\mathbf{n}_i^{(t)}\|^2] \leq \sigma^2 \forall i, t$.

ASSUMPTION 2 (GENERAL CHARACTERISTICS OF LOSS FUNCTIONS [19], [30], [18]). Assumptions applied to loss functions include:

- **Bounded gradient:** The stochastic gradient norm of the loss function $\ell(\cdot)$ is bounded by a constant G , i.e.,

$$\|\widehat{\mathbf{g}}_i^{(t)}\| \leq G, \forall i, t. \quad (20)$$

- **Smoothness:** Each local loss F_i is β -smooth $\forall i \in \mathcal{I}$, i.e.,

$$\|\nabla F_i(\mathbf{w}_1) - \nabla F_i(\mathbf{w}_2)\| \leq \beta \|\mathbf{w}_1 - \mathbf{w}_2\|, \forall \mathbf{w}_1, \mathbf{w}_2 \in \mathbb{R}^M, \quad (21)$$

where $\beta > \mu$. This implies β -smoothness of \bar{F}_c and F as well.

- **Inter-Subnet Gradient Diversity:** The inter-subnet gradient diversity across the device subnets is measured via a non-negative constant ζ such that

$$\|\nabla \bar{F}_c(\mathbf{w}) - \nabla F(\mathbf{w})\| \leq \zeta, \forall c, \mathbf{w}. \quad (22)$$

- **Intra-Subnet Gradient Diversity:** The intra-subnet gradient diversity across the devices belonging to subnet \mathcal{S}_c is measured via a non-negative constant ζ_c such that

$$\|\nabla F_i(\mathbf{w}) - \nabla \bar{F}_c(\mathbf{w})\| \leq \zeta_c, \forall i \in \mathcal{S}_c, \forall c, \mathbf{w}. \quad (23)$$

4.2 Preliminary Quantities and Results

Before proceeding to our main result in Sec. 4.3, we establish a few quantities and lemmas to facilitate our analysis.

Auxiliary models: We define the *auxiliary local aggregated model*¹ as

$$\bar{\mathbf{w}}_c^{(t+1)} = \bar{\mathbf{w}}_c^{(t)} - \eta_k \sum_{j \in \mathcal{S}_c} \rho_{j,c} \widehat{\mathbf{g}}_j^{(t)} + \Theta_c^{(t+1)} \bar{\mathbf{n}}_{c,Loc}^{(t+1)}, \forall t \in \mathcal{T}_k \setminus \{t_k\}. \quad (24)$$

Similarly, we define a *auxiliary global model* within each local model training interval preceding the global aggregation as

$$\begin{aligned}\bar{\mathbf{w}}^{(t+1)} &= \bar{\mathbf{w}}^{(t)} - \eta_k \sum_{c=1}^N \varrho_c \sum_{j \in \mathcal{S}_c} \rho_{j,c} \widehat{\mathbf{g}}_j^{(t)} \\ &\quad + \sum_{c=1}^N \varrho_c \Theta_c^{(t+1)} \bar{\mathbf{n}}_{c,Loc}^{(t+1)}, \forall t \in \mathcal{T}_k \setminus \{t_k\}.\end{aligned}\quad (25)$$

The auxiliary global model at the instant of the global aggregation can then be expressed as

$$\bar{\mathbf{w}}^{(t_{k+1})} = \widetilde{\mathbf{w}}^{(t_{k+1})} + \Theta_c^{(t_{k+1})} \bar{\mathbf{n}}_{Glob}^{(t_{k+1})}, \quad (26)$$

where $\widetilde{\mathbf{w}}^{(t_{k+1})}$ is the auxiliary global model just before global aggregation, distinguishing it from $\bar{\mathbf{w}}^{(t_{k+1})}$, which is defined immediately post global aggregation.

Edge server security probability. We consider a generic probability $p_c \in [0, 1]$ that each subnet is associated with a secure edge server, and a probability $1 - p_c$ that it is associated with an insecure one. Consequently, $\bar{\mathbf{n}}_{c,Loc}^{(t)}$ is a mixture model:

$$\bar{\mathbf{n}}_{c,Loc}^{(t)} = \begin{cases} \bar{\mathbf{n}}_{c,Loc}^{(t)}, & \text{with probability } p_c, \\ \sum_{j \in \mathcal{S}_c} \rho_{j,c} \mathbf{n}_{j,Loc}^{(t)}, & \text{with probability } 1 - p_c. \end{cases} \quad (27)$$

In what follows, for ease of presentation, we assume that $K_{k,c} = K_\ell$ (the number of local aggregations within \mathcal{T}_k), $\tau_k = \tau$ (the duration of the local model training interval), and $s_c^k = s_c$ (the size of cluster c) are constant for k, c . The control algorithm in Algorithm 1 will facilitate adaptation of these parameters across k and c through a re-optimization after each local training interval.

Model dispersion. We next introduce a series of terms that encapsulate model characteristics within and across subnets.

(i) *Expected intra-subnet model dispersion:* We define

$$Z_1^{(t)} \triangleq \mathbb{E} \left[\sum_{c=1}^N \varrho_c \sum_{j \in \mathcal{S}_c} \rho_{j,c} \|\mathbf{w}_j^{(t)} - \bar{\mathbf{w}}_c^{(t)}\|^2 \right] \quad (28)$$

to capture the average deviation error of local models $\mathbf{w}_i^{(t)}$ within a subnet from the local aggregated model $\bar{\mathbf{w}}_c^{(t)}$.

(ii) *Expected inter-subnet model dispersion:* Similarly,

$$Z_2^{(t)} \triangleq \mathbb{E} \left[\sum_{c=1}^N \varrho_c \|\bar{\mathbf{w}}_c^{(t)} - \bar{\mathbf{w}}^{(t)}\|^2 \right]. \quad (29)$$

measures the degree to which the local aggregated $\bar{\mathbf{w}}_c^{(t)}$ deviates from the global model $\bar{\mathbf{w}}^{(t)}$ during the local training interval.

¹“Auxiliary” refers to $\bar{\mathbf{w}}_c^{(t)}$ only being realized at the edge server upon performing a local aggregation at $t \in \mathcal{T}_{k,c}^L$. Similarly, $\bar{\mathbf{w}}^{(t)}$ is realized upon executing global aggregations at $t = t_{k+1}, \forall k$.

LEMMA 4.1 (ONE-STEP BEHAVIOR OF INTRA/INTER SUBNET MODEL DEVIATION). For $t \in \mathcal{T}_k \setminus \{t_{k+1}\}$, under Assumptions 1 and 2, the one-step behavior of $\sqrt{\mathbb{E}[\|\mathbf{e}_i^{(t)}\|^2]}$ and $\sqrt{\mathbb{E}[\|\bar{\mathbf{w}}_c^{(t)} - \bar{\mathbf{w}}^{(t)}\|^2]}$ follows

$$\begin{aligned} \sqrt{\mathbb{E}[\|\mathbf{e}_i^{(t+1)}\|^2]} &\leq (1 - \Theta_c^{(t+1)}) \left[(1 + \eta_k \beta) \sqrt{\mathbb{E}[\|\mathbf{e}_i^{(t)}\|^2]} \right. \\ &\quad \left. + \eta_k \beta \sum_{j \in \mathcal{S}_c} \rho_{j,c} \sqrt{\mathbb{E}[\|\mathbf{e}_i^{(t)}\|^2]} + \eta_k (2\sigma + \zeta_c) \right], \end{aligned} \quad (30)$$

and

$$\begin{aligned} \sqrt{\mathbb{E}[\|\bar{\mathbf{w}}_c^{(t+1)} - \bar{\mathbf{w}}^{(t+1)}\|^2]} &\leq (1 + \eta_k \beta) \sqrt{\mathbb{E}[\|\bar{\mathbf{w}}_c^{(t)} - \bar{\mathbf{w}}^{(t)}\|^2]} \\ &\quad + \eta_k \beta \sum_{d=1}^N \varrho_d \sqrt{\mathbb{E}[\|\bar{\mathbf{w}}_d^{(t)} - \bar{\mathbf{w}}^{(t)}\|^2]} + \eta_k (2\beta \max_{t \in \mathcal{T}_k} Z_1^{(t)} + 2\sigma + \zeta) \\ &\quad + \sqrt{M \sum_{d=1}^N \varrho_d^2 \Theta_d^{(t+1)} (p_d \bar{\sigma}_{Loc}^2 + (1 - p_d) \sigma_{Loc}^2 \sum_{j \in \mathcal{S}_d} \rho_{j,d}^2)} \\ &\quad + \Theta_c^{(t+1)} \sqrt{M (p_c \bar{\sigma}_{Loc}^2 + (1 - p_c) \sigma_{Loc}^2 \sum_{j \in \mathcal{S}_c} \rho_{j,c}^2)}. \end{aligned} \quad (31)$$

Lemma 4.1 elucidates the one-step dynamics of $\sqrt{\mathbb{E}[\|\mathbf{e}_i^{(t+1)}\|^2]}$ and $\sqrt{\mathbb{E}[\|\bar{\mathbf{w}}_c^{(t+1)} - \bar{\mathbf{w}}^{(t+1)}\|^2]}$ within a local model training interval at t . These upper bounds indicate a complex interplay between $\sqrt{\mathbb{E}[\|\mathbf{e}_i^{(t+1)}\|^2]}$ and $\sqrt{\mathbb{E}[\|\bar{\mathbf{w}}_c^{(t+1)} - \bar{\mathbf{w}}^{(t+1)}\|^2]}$ when local model updates are conducted within H²FDP. Specifically, when local aggregation is carried out, $\Theta_c^{(t+1)} = 1$, thus bringing $\sqrt{\mathbb{E}[\|\mathbf{e}_i^{(t+1)}\|^2]} = 0$. While this decreases $\sqrt{\mathbb{E}[\|\bar{\mathbf{w}}_c^{(t+1)} - \bar{\mathbf{w}}^{(t+1)}\|^2]}$ on the one hand by reducing the values of $Z_1^{(t)}$, it simultaneously inflates it due to the injection of DP noise. This leads us to the following proposition:

PROPOSITION 4.2. For $t \in \mathcal{T}_k \setminus \{t_{k+1}\}$, under Assumptions 1 and 2, if $\eta_k \leq \frac{1}{\max\{\tau, K_g\} \beta}$, the subnet model dispersion can be bounded as

$$Z_1^{(t)} \leq \eta_k \tau B_1^2, \quad Z_2^{(t)} \leq \eta_k \tau B_2^2, \quad (32)$$

where $B_1^2 = (2\sigma + \zeta_c)^2 \left((1 + 2\eta_0 \beta)^{\tau-1} + 1 \right)^2$, $B_2^2 = (1 + \eta_0 \beta)^2 (\tau-1) \sum_{c=1}^N \varrho_c \Phi_c^2$,

$$\begin{aligned} \text{and } \Phi_c &= \left[\frac{2\tau G q \sqrt{MK_f \log(\frac{1}{\delta})}}{\varepsilon N} \left(\sqrt{\sum_{c=1}^N (p_c \frac{c_2^2}{s_c^2} + (1 - p_c) \frac{\sigma_2^2}{s_c})} \right. \right. \\ &\quad \left. \left. + N \sqrt{p_c \frac{c_2^2}{s_c^2} + (1 - p_c) \frac{\sigma_2^2}{s_c}} \right) + 2B_1^2 + 2\sigma + \zeta \right] \\ &\quad \times \left((1 + 2\eta_0 \beta)^{\tau-1} + 1 \right) + 2B_1^2 + 2\sigma + \zeta. \end{aligned}$$

Proposition 4.2 offers a viewpoint on how subnet configuration impacts the convergence trajectory of the model training process, by establishing bounds on the subnet deviation parameters, $Z_1^{(t)}$ and $Z_2^{(t)}$. It highlights how SGD noise and intra-subnet data diversity, encapsulated within B_1 and B_2 , influence the bounds. Specifically, it indicates an upward shift in the bound from increasing σ , ζ_c , and ζ . Moreover, the proposition indicates that the network size, both in terms of individual subnet size, i.e., s_c , and total number of subnets, i.e., N , significantly influences these bounds and, in turn, model convergence dynamics. In particular, it reveals an inverse

relationship: a larger network results in the need for less DP noise injection, which in turn results in a decrease in model dispersion.

Furthermore, Proposition 4.2 illustrates that the progression of the upper bounds of $Z_1^{(t)}$ and $Z_2^{(t)}$ across sequential global synchronization stages is proportional to the step size. This relationship is instrumental in steering the convergence pattern of the global model within the H²FDP framework, which we establish next.

4.3 General Convergence Behavior of H²FDP

We now present our main theoretical result, that the cumulative average of the global loss gradient can attain sublinear convergence to a controllable region around a stationary point.

THEOREM 4.3. Under Assumptions 1 and 2, if $\eta_k = \frac{\gamma}{\sqrt{k+1}}$ with $\gamma \leq \min\{\frac{1}{\tau}, \frac{1}{K_g}\} / \beta$, the cumulative average of global gradient satisfies

$$\begin{aligned} \frac{1}{K_g} \sum_{k=0}^{K_g-1} \mathbb{E}[\|\nabla F(\bar{\mathbf{w}}^{(t_k)})\|^2] &\leq 2\gamma \underbrace{\frac{F(\bar{\mathbf{w}}^{(0)}) - F(\mathbf{w}^*)}{\tau \sqrt{K_g + 1}}}_{(a_1)} \\ &\quad + \underbrace{\frac{\beta \gamma}{\sqrt{K_g + 1}} \left[\beta \tau (B_1^2 + B_2^2) + G^2 + \tau \sigma^2 \right]}_{(a_2)} \\ &\quad + \underbrace{\frac{4\tau(K_f^3 + 1)Mq^2G^2 \log(1/\delta)}{N^2 \varepsilon^2} \sum_{c=1}^N \left(p_c \frac{c_2^2}{s_c^2} + (1 - p_c) \frac{\sigma_2^2}{s_c} \right)}_{(b)}. \end{aligned} \quad (33)$$

Noise injection creates a delicate balance between privacy conservation and model performance: as the number of global aggregations (K_g) increases, (a₁) and (a₂) in (33) decrease, while the overall noise level in (b) escalates. As suggested by Proposition 3.1 and Lemma 3.2, the variance of the DP noise inserted should scale with the total count of global aggregations, K_g . To counterbalance the influence of DP noise accumulation over successive aggregations, we enforce the condition $\eta_k \leq 1/K_g$ to scale down the DP noise by a factor of K_g . This strategy steers the bound in (33) towards the region denoted by (b), rather than allowing for constant amplification. At the same time, this highlights the trade-off between privacy preservation and model performance: although the condition $\eta_k \leq 1/K_g$ serves to reduce DP noise, it simultaneously results in a smaller learning rate which slows H²FDP training.

In addition, (b) conveys the beneficial influence of secure edge servers. With more such servers (indicated by a larger p_c), the noise level introduced during aggregations is reduced by a factor of $1/s_c^2$. This is in contrast to a factor of $1/s_c$ for the noise introduced at insecure edge servers, resulting in an additional noise reduction by a factor of s_c . This reduction underscores the rationale behind H²-FDP's integration of HDP with HFL, allowing for an effective reduction in the requisite DP noise for preserving a given privacy level. Consequently, in comparison with hierarchical FL implementing the LDP strategy [20] – tantamount to setting $p_c = 0$ in (33) – H²FDP noticeably suppresses the noise impact by an extra factor

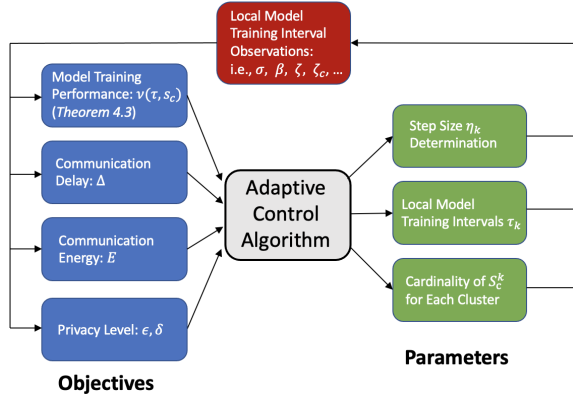


FIGURE 3: Overview of the adaptive control algorithm, outlining its objectives, adjustable parameters, and observations.

of $1/s_c$. Our bound subsumes many other existing results in DP-enhanced FL as well, e.g., if both $p_c = 0$ and $B_1 = 0$, we recover LDP in a non-hierarchical, star-topology FL system [19].

Lastly, the network size, represented by the number of subnets N and the size of each subnet s_c , is inversely related to the DP noise needed to uphold a specific privacy level. Specifically, a rise in either N or s_c sees (b) decrease.

5 ADAPTIVE CONTROL ALGORITHM

Our control algorithm framework is summarized in Fig. 3. The algorithm specifically targets three key adjustable parameters within H^2 -FDP: (P1) the size of the gradient descent step $\{\eta_k\}$, (P2) the number of active devices in each cluster $\{s_c^k\}$, and (P3) the length of local model training intervals $\{\tau_k\}$. The central server orchestrates these parameters during the global aggregation step at $t = t_k$, $\forall k$. We assume the network operator will specify (i) desired (ϵ, δ) privacy requirements, (ii) a target number of global aggregations K_g , and (iii) the number of local aggregations K_ℓ per training interval k .

Our control algorithm has two parts: *Part I* employs an adaptive approach (detailed in Sec. 5.1) for calibrating the step-size to ensure the convergence performance from Theorem 4.3. *Part II* adopts an optimization framework (outlined in Sec. 5.2) to adapt s_c^k and τ_k , balancing the objectives of ML accuracy and resource consumption for the target DP requirement.

5.1 Step Size Parameters (γ_k)

We begin by fine-tuning the step size parameter γ_k , taking into account the relevant measures β , K_g , and τ . The server is tasked with estimating β , for which we follow Section IV-C of [11]. K_g is pre-specified. τ is either taken as τ_{k-1} from the previous interval, or initialized for the first interval \mathcal{T}_0 . Given that higher feasible γ_k values enhance the step sizes, leading to faster model convergence as per the conditions described in Theorem 4.3, we identify the maximum γ_k value that complies with $\gamma_k \leq \min\{\frac{1}{\tau_{k-1}}, \frac{1}{K_g}\}/\beta$.

5.2 Training Interval (τ_k) and Participation (s_c^k)

Building upon the initial adjustment of step size parameters, we proceed to craft an optimization problem \mathcal{P} that determines τ_k and $\{s_c^k\}_{c=1}^N$. \mathcal{P} is designed to jointly optimize three competing

objectives: (O1) the energy consumption associated with local and global model aggregations, (O2) the communication delays incurred during these aggregations, and (O3) the performance of the global model, taking into account the impact of the DP noise injection procedure in H^2 -FDP dictated by Theorem 4.3. Formally, we have:

$$\begin{aligned}
 (\mathcal{P}) : \quad & \min_{\tau_k, \{s_c^k\}_{c=1}^N} \underbrace{\alpha_1 \left(\frac{T-t_k}{\tau_k} \right) \left(E_{\text{Glob}}(\{s_c^k\}) + K_\ell \sum_{c=1}^N E_{c,\text{Loc}}(s_c^k) \right)}_{(a)} \\
 & \underbrace{\alpha_2 \left(\frac{T-t_k}{\tau_k} \right) \left(\Delta_{\text{Glob}}(\{s_c^k\}) + K_\ell \sum_{c=1}^N \Delta_{c,\text{Loc}}(s_c^k) \right)}_{(b)} + \underbrace{\alpha_3 v(\tau_k, \{s_c^k\})/\phi}_{(c)}
 \end{aligned}$$

$$\text{subject to } 1 \leq \tau_k \leq \min\{\tau_{\text{max}}, T-t_k\}, \tau \in \mathbb{Z}^+, \quad (34)$$

$$0 \leq s_c^k \leq s_c, s_c^k \in \mathbb{Z}^+. \quad (35)$$

Objectives: Term (a) captures the communication energy expenditure over the estimated remaining global aggregations. The energy consumption from local model aggregation at an edge server, denoted as $E_{c,\text{Loc}}$, is calculated by summing up the energy used by the selected devices $\mathcal{S}_c^k \in \mathcal{S}_c$ from cluster c . Similarly, the global aggregation energy consumption, E_{Glob} , accumulates the energy used for communications between all edge servers and the main server. We employ standard wireless energy transmission models here, which we present in Appendix D as they boil down to scaling factors on the variables s_c^k in \mathcal{P} . Term (b), on the other hand, captures communication delay incurred over the estimated remaining local intervals. The delay for local aggregation, $\Delta_{c,\text{Loc}}$, captures the total consumed time it takes for all selected devices in cluster c to transmit the model updates based on their transmission rates. The global aggregation delay, denoted as Δ_{Glob} , represents the sum of round-trip communication time between all selected devices and the main server. We again employ standard wireless delay models here, deferred to Appendix D. Finally, term (c) represents the upper bound on the optimality gap – quantified as term (b) in Theorem 4.3 – evaluated at $t = t_{k-1} + \tau_k$. A lower value is thus in line with better ML performance.²

Constraints: Constraint (34) ensures that the value of τ_k remains within a preset range, i.e., to prevent any given local training interval from becoming too long. Meanwhile, (35) ensures that the number of participating devices in each cluster does not exceed the cluster size. Increasing s_c^k will hinder the energy and delay objectives, while from Theorem 4.3, we see that it will improve the stationarity gap objective term (c). The value of τ_k has the opposite effect, as increasing it causes the stationarity gap to grow, but simultaneously reduces the frequency of aggregations.

Solution: \mathcal{P} is classified as a non-convex mixed-integer programming problem due to term (c). For our experiments, we employ a nested line search strategy to tackle this problem. Despite this method, the total time complexity is $O(N\tau_{\text{max}} \times s_{\text{max}})$, and computational complexity increases with the network size, i.e., N . To mitigate this, we simplify the decision variable space by reducing it from N to just 2, categorizing by cluster sizes associated with

²The scaling factor ϕ is introduced to keep $\alpha_1, \alpha_2, \alpha_3$ in a similar range since the value of $v(\cdot)$ tends to be substantially larger than the values for terms (a) and (b) in practice.

Algorithm 1: H^2 -FDP with adaptive control parameters.

Input: Number of global aggregations K_g , minibatch sizes $|\zeta_i^{(t)}|$, privacy level ϵ , δ
Output: Global model $\bar{w}^{(T)}$

- 1 Initialize $\bar{w}^{(0)}$ and broadcast it among the edge devices through the edge server.
- 2 Initialize estimates of $\hat{\beta}$, $\hat{\sigma}$, $\hat{\zeta}$, $\hat{\zeta}_c$.
- 3 Initialize $t = 0$, $k = 0$, $t_0 = 0$, $t_1 = \tau_0$, with τ_0 chosen randomly, such that $\tau_0 \leq T - t_k$, $\forall k$.
- 4 Initialize $\gamma \leq \min\{\frac{1}{t_0}, \frac{1}{K_g}\}/\beta$ for the step size according to Sec. 5.1.
- 5 **while** $t \leq T$ **do**
- 6 **while** $t \leq t_{k+1}$ **do**
- 7 **for** $c = 1 : N$ **do** // Operation at the subnets
- 8 Each device $i \in \mathcal{S}_c$ performs a local SGD update based on (7) and (8) using $w_i^{(t-1)}$ to obtain $\tilde{w}_i^{(t)}$.
- 9 **if** $t \in \mathcal{T}_{k,c}^L$ **then**
- 10 **if** $n_c \in \mathcal{N}_T$ **then**
- 11 Edge device i sends accumulated gradients $\eta_k \sum_{\ell=t-m_k}^t \tilde{g}_i^{(\ell)}$ via uplink transmission;
- 12 Edge server n_c conducts local aggregation with:

$$\bar{w}_c^{(t)} = \bar{w}_c^{(t-m_k)} - \eta_k \sum_{\ell=t-m_k}^t \sum_{j \in \mathcal{S}_c} \rho_{j,c} \tilde{g}_j^{(\ell)} + \bar{n}_{c,Loc}^{(t)}$$
and $w_i^{(t)} = \bar{w}_c^{(t)}$;
- 13 **else**
- 14 Edge device i sends noisy accumulated gradients $\eta_k \sum_{\ell=t-m_k}^t \tilde{g}_i^{(\ell)} + n_{i,Loc}^{(t)}$ via uplink transmission;
- 15 Edge server conducts local aggregation with:

$$\bar{w}_c^{(t)} = \bar{w}_c^{(t-m_k)} - \eta_k \sum_{\ell=t-m_k}^t \sum_{j \in \mathcal{S}_c} \rho_{j,c} \tilde{g}_j^{(\ell)} + \sum_{j \in \mathcal{S}_c} \rho_{j,c} n_{j,Loc}^{(t)}$$
and $w_i^{(t)} = \bar{w}_c^{(t)}$;
- 16 **else**
- 17 $w_i^{(t)} = \tilde{w}_i^{(t)}$.
- 18 **if** $t = t_{k+1}$ **then**
- 19 // Operation at the edge server
- 20 **for** $c = 1 : N$ **do** // Procedure at each subnet \mathcal{S}_c
- 21 **if** $n_c \in \mathcal{N}_T$ **then**
- 22 Edge device i sends accumulated gradients $\eta_k \sum_{\ell=t-m_k}^t \tilde{g}_i^{(\ell)}$ via uplink transmission;
- 23 Edge server n_c computes and sends $\eta_k \sum_{\ell=t-m_k}^t \sum_{j \in \mathcal{S}_c} \rho_{j,c} \tilde{g}_j^{(\ell)} + \bar{n}_{c,Glob}^{(t)}$ via uplink transmission;
- 24 **else**
- 25 Edge device i sends noisy accumulated gradients $\eta_k \sum_{\ell=t-m_k}^t \tilde{g}_i^{(\ell)} + n_{i,Glob}^{(t)}$ via uplink transmission;
- 26 Edge server computes and sends $\eta_k \sum_{\ell=t-m_k}^t \sum_{j \in \mathcal{S}_c} \rho_{j,c} \tilde{g}_j^{(\ell)} + \sum_{j \in \mathcal{S}_c} \rho_{j,c} n_{j,Glob}^{(t)}$ via uplink transmission;
- 27 // Operation at the edge server
- 28 Compute $\bar{w}^{(t_{k+1})}$ according to (14).
- 29 Estimate $\hat{\beta}_k$, $\hat{\sigma}_k$, $\hat{\zeta}_k$ and $\hat{\zeta}_{c,k}$ using the method in [11].
- 30 Characterize γ for the step size $\eta_k = \frac{\gamma}{\sqrt{k+1}}$ according to Sec. 5.1.
- 31 Solve the optimization \mathcal{P} to obtain τ_{k+1} and $\{\mathcal{S}_c\}_{c=1}^N$.
- 32 Broadcast (i) $\bar{w}^{(t_{k+1})}$, (ii) $\{\mathcal{S}_c\}_{c=1}^N$ and (iii) η_k among the devices.
- 33 $t \leftarrow t + 1$
- 34 $k \leftarrow k + 1$ and $t_{k+1} \leftarrow t_k + \tau_k$

secure (i.e., $n_c \in \mathcal{N}_T$) and insecure (i.e., $n_c \in \mathcal{N}_U$) edge servers. This reduction is based on the observation that clusters served by the same type of server exhibit similar behaviors. Consequently, this approach significantly narrows the search space for \mathcal{P} , making the computational task more manageable, with line search complexities of $\mathcal{O}(\max\{T - t_k, \tau\})$ for τ and $\mathcal{O}(s_{max})$ for s_c .

The overall control algorithm is summarized in Algorithm 1.

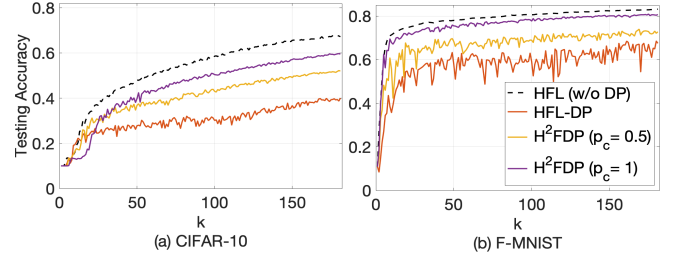


FIGURE 4: Performance comparison between H^2 FDP, the HFL-DP baseline from [20], and an upper bound established by hierarchical FedAvg without DP. H^2 FDP significantly outperforms HFL-DP and is able to leverage trusted edge servers effectively.

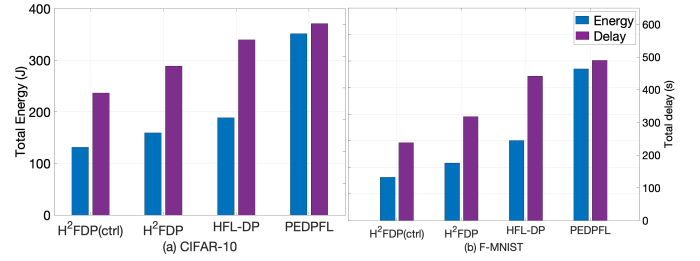


FIGURE 5: Comparison of H^2 FDP with adaptive parameter control (Alg. 1) to the baselines in total energy and delay upon reaching 75% testing accuracy. H^2 FDP obtains substantial improvements in both metrics for both F-MNIST and CIFAR-10.

6 EXPERIMENTAL EVALUATION

6.1 Simulation Setup

By default, we consider a network of 50 edge devices evenly distributed across 10 subnets. We use two commonly employed datasets for image classification tasks: Fashion-MNIST (F-MNIST) and CIFAR-10. Following prior work [11, 25], the training samples from each dataset are distributed across the edge devices in a non-i.i.d manner, in which each device exclusively contains datapoints from 3 out of 10 labels. For each dataset, we consider training a 12-layer convolutional neural network (CNN) accompanied by a softmax function and cross-entropy loss. The model dimension is set to $M = 7840$. This evaluation setup provides insight into H^2 FDP's performance when handling non-convex loss functions. Also, unless otherwise stated, we assume $p_c = 0.5$, and that semi-honest entities are all governed by the same total privacy budget $\epsilon = 1$, $\delta = 10^{-5}$.

The control algorithm parameters, including its energy and delay models, are deferred to Appendix D.

6.2 H^2 FDP Comparison to Baselines

Our first experiments examine the performance of H^2 FDP compared with baselines. We utilize the conventional hierarchical FedAvg algorithm [13], which offers no explicit privacy protection, as our upper bound on achievable accuracy (labeled HFL (w/o DP)). We also implement HFL-DP [20], which employs LDP within the hierarchical structure, for competitive analysis. Further, we consider PEDPFL [19], a DP-enhanced FL approach developed for the standard star-topology structure, for which we assume the edge devices all form a single cluster and apply LDP.

6.2.1 Training Convergence Performance. Fig. 4 demonstrates results comparing H^2FDP without control to baselines. Each algorithm employs a local model training interval of $\tau_k = 20$ and conduct local aggregations after every five local SGD iterations. We see H^2FDP obtains performance enhancements over HFL-DP by exploiting secure edge servers in the hierarchical architecture’s middle-layer. This improvement is observed both in terms of superior testing accuracy and decreased accuracy perturbation as the probability (p_c) of a subnet being linked to a secure edge server escalates. Specifically, when $p_c = 0.5$, H^2FDP achieves an accuracy gain at $k = 200$ of 12% and 6% for CIFAR-10 and F-MNIST, respectively, and displays reduced volatility in the accuracy curve compared to HFL-DP. When all subnets are linked to a secure edge server ($p_c = 1$), the improvement almost doubles. Notably, compared to the upper bound benchmark, H^2FDP with $p_c = 1$ achieves an accuracy within 8% and 3% of the benchmark for CIFAR-10 and F-MNIST, respectively. The exploitation of secure edge servers into the middle-layer of the hierarchy significantly mitigates the amount of noise required to maintain an equivalent privacy level.

6.2.2 Adaptive Control Algorithm Performance. Next, we evaluate H^2FDP ’s control algorithm performance. Fig. 5 demonstrates the results, where the total energy consumption (O1) and total delay (O2) are assessed upon the global model achieving a testing accuracy of 75%. Overall, we see that H^2FDP with control (ctr1) substantially improves over the baselines for both metrics. For (O1), the blue bars show reductions in energy consumption by 17.6% and 25.1% compared to H^2FDP without control, by 30.3% and 46.2% compared to HFL-DP, and by 62.6% and 71.5% compared to PEDPFL for the CIFAR-10 and FMNIST datasets, respectively. Similarly, for (O2), the red bars indicate that H^2FDP (ctr1)’s delay is 18.1% and 24.9.1% less than H^2FDP without control, 30.1% and 43.2% less than HFL-DP, and 36.2% and 51.3% less than PEDPFL for the CIFAR-10 and FMNIST datasets. These results highlight the enhanced performance and efficiency in resource usage offered by H^2FDP through its adaptive parameter control, which optimizes the balance between the optimality gap (as established in Theorem 4.3), communication delay, and energy consumption. Notably, the improvement in both metrics underscores the advantage of the joint device participation and training interval optimization strategy employed by H^2FDP .

6.3 Impact of System Parameters

6.3.1 Portion of Secure Edge Servers. We next consider the impact of the probability p_c of a subnet having a secure edge server. Fig. 6 shows that H^2FDP obtains a considerable enhancement in privacy-performance tradeoff as the probability escalates. Specifically, under the same privacy conditions, H^2FDP exhibits an improvement of at least 20% for CIFAR-10 and 10% for F-MNIST when all the edge servers in the mid-layer can be trusted (i.e., $p_c = 1$) compared to HFL-DP (i.e., $p_c = 0$). For instance, when $p_c = 1$ and $\epsilon = 0.5$, H^2FDP achieves accuracy boosts of 40% for CIFAR-10 and 25% for F-MNIST.

6.3.2 Varying Network Configurations. Next, we investigate the impact of different network configurations on the performance of H^2FDP . Two distinct configurations are evaluated: (i) Config. 1, wherein the size of subnets (s_c) is kept at 5 as the number of subnets (N) increases from 2 to 10; (ii) Config. 2, wherein N is fixed at 2,

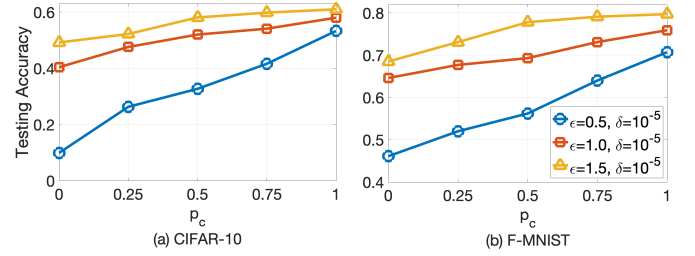


FIGURE 6: Interplay between privacy and performance in H^2FDP across various probabilities (p_c) of a subnet’s linkage to a secure edge server under different privacy budgets (ϵ).

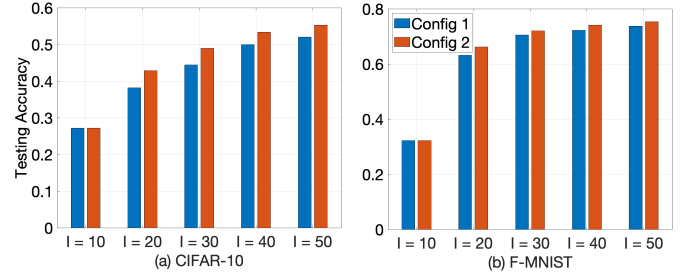


FIGURE 7: Impact of various network configurations on the performance of H^2FDP . Under the same network size, enhancing the size of each subnet s_c yields superior test accuracy compared to merely increasing the number of subnets N .

and s_c increases from 5 to 25. Fig. 7 gives the results. The positive correlation between network size and model performance is apparent in both configurations: specifically, the accuracy gain can be as substantial as 25% and 42% for CIFAR-10 and F-MNIST, respectively, when the network size transitions from $I = 10$ to $I = 50$. This can be attributed to the diminishing contribution of individual devices in aggregations. This observation aligns well with Theorem 4.3, which quantifies the noise reduction as the network size expands.

Also, Config. 2 leads to superior model performance compared to Config. 1: even while retaining the same network size, model performance sees an uptick as the size of each subnet amplifies, which is more beneficial than solely increasing the number of subnets. This pattern once again aligns with Theorem 4.3: when subnets are linked to a secure edge server, the extra noise needed to maintain an equivalent privacy level during aggregations can be downscaled by $1/s_c^2$, which is generally more pronounced than the reduction achieved through the augmentation of the subnet number, i.e., $1/N$.

6.3.3 Objective Weights in \mathcal{P} . Fig. 8 investigates the control algorithm’s response to varying optimization weights in \mathcal{P} . In this experiment, we set $\tau_{max} = 40$ and $\max\{s_c\} = 15$, and use the F-MNIST dataset. The plotted values of τ_k and s_c^k are averaged over the entire training process. We see that an increase in α_1 , the weight on communication energy, results in (i) extended training intervals τ , attributed to less frequent global aggregations cutting down on communications, and (ii) a decreased count s_c of devices engaged in training, thereby reducing communication overhead.³ In contrast, increasing α_3 , the weight on the ML performance, leads to (i) more

³The effects of α_1 and α_2 on the decision variable are comparable. The results for α_2 are deferred to Appendix E.

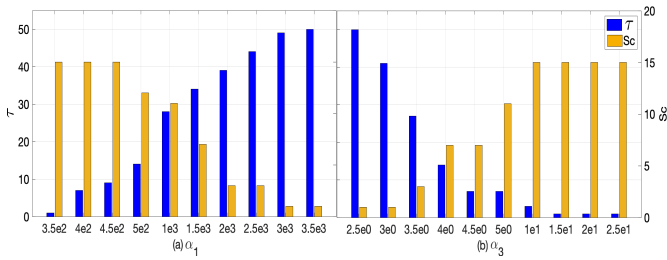


FIGURE 8: Average values of τ_k and S_c^k chosen by Algorithm 1 across various configurations of coefficients α_1 and α_3 .

frequent global aggregations, reducing extensive intervals of local training that could lead to biased local models, and (ii) augments the number of devices participating in training, leveraging a larger pool of training data for enhanced learning performance.

7 CONCLUSION

In this study, we developed H^2FDP , which integrates hierarchical differential privacy (HDP) into hierarchical federated learning (HFL) to enhance the trade-off between privacy and performance. We conducted a thorough theoretical analysis of H^2FDP , identifying conditions under which the algorithm will converge sublinearly to a controllable region around a stationary point, and revealing the impact of different system factors on the privacy-utility trade-off. Based on our analysis, we developed an adaptive control algorithm to jointly optimize communication energy, latency, and the stationarity gap while enforcing the sub-linear rate and meeting desired privacy requirements. Numerical evaluations confirmed H^2FDP 's superior training performance and improvements in resource efficiency compared to existing DP-infused FL/HFL algorithms.

REFERENCES

- [1] Martin Abadi, Andy Chu, Ian Goodfellow, H. Brendan McMahan, Ilya Mironov, Kunal Talwar, and Li Zhang. 2016. Deep Learning with Differential Privacy. In *Proc. Conf. on Comput. Commun. Security (SIGSAC)*, Vol. 24. Association for Computing Machinery, 308–318.
- [2] Mohammad Al-Rubaie and J. Morris Chang. 2019. Privacy-Preserving Machine Learning: Threats and Solutions. *IEEE Security Privacy* 17, 2 (2019), 49–58.
- [3] Varun Chandrasekaran, Suman Banerjee, Diego Perino, and Nicolas Kourtellis. 2022. Hierarchical Federated Learning with Privacy. *arXiv:2206.05209* (2022).
- [4] Yun-Wei Chu, Seyyedali Hosseinalipour, Elizabeth Tenorio, Laura Cruz, Kerrie Anna Douglas, Andrew S. Lan, and Christopher G. Brinton. 2022. Mitigating Biases in Student Performance Prediction via Attention-Based Personalized Federated Learning. *Proc. ACM Int. Conf. Inf. Knowl. Manag.* (2022).
- [5] Emiliano De Cristofaro. 2021. A Critical Overview of Privacy in Machine Learning. *IEEE Security Privacy* 19, 4 (2021), 19–27.
- [6] Cynthia Dwork and Aaron Roth. 2014. The algorithmic foundations of differential privacy. 9, 3-4 (2014), 211–407.
- [7] Farhad Farokhi, Nan Wu, David Smith, and Mohamed Ali Kaafar. 2021. The Cost of Privacy in Asynchronous Differentially-Private Machine Learning. *IEEE Trans. Inf. Forensics Security* 16 (2021), 2118–2129.
- [8] Farzin Haddadpour and Mehrdad Mahdavi. 2019. On the convergence of local descent methods in federated learning. *arXiv:1910.14425* (2019).
- [9] Seyyedali Hosseinalipour, Sheikh Azam, Christopher Brinton, Nicolò Michelusi, Vaneet Aggarwal, David Love, and Huaiyu Dai. 2022. Multi-Stage Hybrid Federated Learning Over Large-Scale D2D-Enabled Fog Networks. *IEEE/ACM Trans. Netw.* 30, 4 (2022), 1569–1584.
- [10] Jakub Konečný, H. Brendan McMahan, Felix X. Yu, Peter Richtárik, Ananda Theertha Suresh, and Dave Bacon. 2017. Federated Learning: Strategies for Improving Communication Efficiency. *arXiv:1610.05492* (2017).
- [11] Frank Po-Chen Lin, Seyyedali Hosseinalipour, Sheikh Shams Azam, Christopher G. Brinton, and Nicolo Michelusi. 2021. Semi-Decentralized Federated Learning with Cooperative D2D Local Model Aggregations. *IEEE J. Sel. Areas Commun.* (2021).
- [12] Jiandong Liu, Lan Zhang, Xiaojing Yu, and Xiang-Yang Li. 2023. Differentially Private Distributed Online Convex Optimization Towards Low Regret and Communication Cost (*MobiHoc '23*). Association for Computing Machinery, New York, NY, USA, 171–180.
- [13] Lumin Liu, Jun Zhang, SH Song, and Khaled B Letaief. 2020. Client-edge-cloud hierarchical federated learning. In *Proc. IEEE Int. Conf. Commun. (ICC)*. 1–6.
- [14] H. Brendan McMahan, Eider Moore, Daniel Ramage, Seth Hampson, and Blaise Aguera y Arcas. 2017. Communication-Efficient Learning of Deep Networks from Decentralized Data. In *Proc. Int. Conf. Artificial Intell. Stat. (AISTATS)*.
- [15] Luca Melis, Congzheng Song, Emiliano De Cristofaro, and Vitaly Shmatikov. 2019. Exploiting Unintended Feature Leakage in Collaborative Learning. In *IEEE Symp. Security Privacy (SP)*. 691–706.
- [16] Mohammad Naseri, Jamie Hayes, and Emiliano De Cristofaro. 2022. Local and Central Differential Privacy for Robustness and Privacy in Federated Learning. *arXiv:2009.03561* (2022).
- [17] Jing Qiao, Shikun Shen, Shuzhen Chen, Xiao Zhang, Tian Lan, Xiuzhen Cheng, and Dongxiao Yu. 2023. Communication Resources Limited Decentralized Learning with Privacy Guarantee through Over-the-Air Computation. In *Proceedings of the 24-th International Symposium on Theory, Algorithmic Foundations, and Protocol Design for Mobile Networks and Mobile Computing* (Washington, DC, USA) (*MobiHoc '23*). Association for Computing Machinery, New York, NY, USA, 201–210.
- [18] Sashank J. Reddi, Zachary Charles, Manzil Zaheer, Zachary Garrett, Keith Rush, Jakub Konečný, Sanjiv Kumar, and Hugh Brendan McMahan. 2021. Adaptive Federated Optimization. In *Proc. Int. Conf. Learn. Representations*.
- [19] Xicong Shen, Ying Liu, and Zhaoyang Zhang. 2022. Performance-Enhanced Federated Learning With Differential Privacy for Internet of Things. *IEEE Internet Things J.* 9, 23 (2022), 24079–24094.
- [20] Lu Shi, Jiangang Shu, Weizhe Zhang, and Yang Liu. 2021. HFL-DP: Hierarchical Federated Learning with Differential Privacy. In *Proc. IEEE Int. Glob. Commun. Conf. (GLOBECOM)*. 1–7.
- [21] Peng Sun, Xu Chen, Guocheng Liao, and Jianwei Huang. 2022. A Profit-Maximizing Model Marketplace with Differentially Private Federated Learning. In *IEEE Conf. Comput. Commun. (INFOCOM)*. 1439–1448.
- [22] David Tse and Pramod Viswanath. 2005. *Fundamentals of wireless communication*. Cambridge university press.
- [23] Aidmar Wainakh, Alejandro Sanchez Guinea, Tim Grube, and Max Mühlhäuser. 2020. Enhancing Privacy via Hierarchical Federated Learning. In *Workshop IEEE European Symp. Security Privacy (EuroSPW)*. 344–347.
- [24] Junxiao Wang, Song Guo, Xin Xie, and Heng Qi. 2022. Protect Privacy from Gradient Leakage Attack in Federated Learning. In *IEEE Conf. Comput. Commun. (INFOCOM)*. 580–589.
- [25] Shiqiang Wang, Tiffany Tuor, Theodoros Salonidis, Kin K Leung, Christian Makaya, Ting He, and Kevin Chan. 2019. Adaptive federated learning in resource constrained edge computing systems. *IEEE J. Select. Areas Commun.* 37, 6 (2019), 1205–1221.
- [26] Zhibo Wang, Mengkai Song, Zhifei Zhang, Yang Song, Qian Wang, and Hairong Qi. 2019. Beyond Inferring Class Representatives: User-Level Privacy Leakage From Federated Learning. In *Proc. IEEE Int. Conf. Comput. Commun. (INFOCOM)*. 2512–2520.
- [27] Kang Wei, Jun Li, Ming Ding, Chuan Ma, Howard H. Yang, Farhad Farokhi, Shi Jin, Tony Q. S. Quek, and H. Vincent Poor. 2020. Federated Learning With Differential Privacy: Algorithms and Performance Analysis. *IEEE Trans. Inf. Forensics Security* 15 (2020), 3454–3469.
- [28] Wenqi Wei, Ling Liu, Margaret L. Loper, Ka Ho Chow, Mehmet Emre Gursoy, Stacey Truex, and Yanzhao Wu. 2020. A Framework for Evaluating Client Privacy Leakages in Federated Learning. In *Computer Security (ESORICS)*. 545–566.
- [29] Zuobin Xiong, Zhipeng Cai, Daniel Takabi, and Wei Li. 2022. Privacy Threat and Defense for Federated Learning With Non-i.i.d. Data in AIoT. *IEEE Trans. Ind. Informat.* 18, 2 (2022), 1310–1321.
- [30] Xinwei Zhang, Xiangyi Chen, Mingyi Hong, Steven Wu, and Jinfeng Yi. 2022. Understanding Clipping for Federated Learning: Convergence and Client-Level Differential Privacy. In *Proc. Machine Learn.*, Vol. 162. 26048–26067.
- [31] Xin Zhang, Minghong Fang, Jia Liu, and Zhengyuan Zhu. 2020. Private and communication-efficient edge learning: a sparse differential gaussian-masking distributed SGD approach (*Mobihoc '20*). Association for Computing Machinery, New York, NY, USA, 261–270.
- [32] Yang Zhao, Jun Zhao, Mengmeng Yang, Teng Wang, Ning Wang, Lingjuan Lyu, Dusit Niyato, and Kwok-Yan Lam. 2021. Local Differential Privacy-Based Federated Learning for Internet of Things. *IEEE Internet Things J.* 8, 11 (2021), 8836–8853.
- [33] Tao Zhou. 2023. Hierarchical Federated Learning with Gaussian Differential Privacy. In *Proc. Int. Conf. Advanced Inf. Sci. Syst.* Article 61, 6 pages.
- [34] Ligeng Zhu, Zhijian Liu, and Song Han. 2019. Deep Leakage from Gradients. In *Proc. Adva. Neural Inf. Process. Syst.*

INTRODUCTION TO NOTATIONS AND PRELIMINARIES USED IN THE PROOFS

We define the auxiliary local aggregated model within each local model training interval before the global aggregation as:

$$\bar{\mathbf{w}}_c^{(t+1)} = \bar{\mathbf{w}}_c^{(t)} - \eta_k \sum_{j \in \mathcal{S}_c} \rho_{j,c} \widehat{\mathbf{g}}_j^{(t)} + \Theta_c^{(t+1)} \bar{\mathbf{n}}_{c,Loc}^{(t+1)}, \quad \forall t \in \mathcal{T}_k \setminus \{t_k\}. \quad (36)$$

Similarly, we define the auxiliary global model within each local model training interval preceding the global aggregation as

$$\bar{\mathbf{w}}^{(t+1)} = \bar{\mathbf{w}}^{(t)} - \eta_k \sum_{c=1}^N \varrho_c \sum_{j \in \mathcal{S}_c} \rho_{j,c} \widehat{\mathbf{g}}_j^{(t)} + \sum_{c=1}^N \varrho_c \Theta_c^{(t+1)} \bar{\mathbf{n}}_{c,Loc}^{(t+1)}, \quad \forall t \in \mathcal{T}_k \setminus \{t_k\}. \quad (37)$$

with the auxiliary global model at global aggregation defined as

$$\bar{\mathbf{w}}^{(t_{k+1})} = \widetilde{\mathbf{w}}^{(t_{k+1})} + \Theta_c^{(t_{k+1})} \bar{\mathbf{n}}_{Glob}^{(t_{k+1})}. \quad (38)$$

Here, $\widetilde{\mathbf{w}}^{(t_{k+1})}$ is the virtual global model just before global aggregation, distinguishing it from $\bar{\mathbf{w}}^{(t_{k+1})}$, which is defined immediately post global aggregation.

A PROOF OF THEOREM A.1

THEOREM A.1. *Under Assumptions 1 and 2, upon using DP-HFL for ML model training, if $\eta_k = \frac{\gamma}{\sqrt{k+1}}$ with $\gamma \leq \min\{\frac{1}{\tau}, \frac{1}{K_g}\}/\beta$, the cumulative average of global loss gradients satisfies*

$$\begin{aligned} \frac{1}{K_g} \sum_{k=0}^{K_g-1} \mathbb{E}[\|\nabla F(\bar{\mathbf{w}}^{(t_k)})\|^2] &\leq 2\gamma \frac{F(\bar{\mathbf{w}}^{(0)}) - F(\mathbf{w}^*)}{\tau\sqrt{K_g+1}} + \frac{\beta\gamma}{\sqrt{K_g+1}} \left[\beta\tau (B_1^2 + B_2^2) + G^2 + \tau\sigma^2 \right] \\ &+ \frac{4\tau(K_\ell^3 + 1)Mg^2G^2 \log(1/\delta)}{N^2\varepsilon^2} \sum_{c=1}^N \left(p_c \frac{c_2^2}{s_c^2} + (1-p_c) \frac{v_c^2}{s_c} \right). \end{aligned}$$

PROOF. Considering $t \in \mathcal{T}_k$, using the definition of $\bar{\mathbf{w}}^{(t_{k+1})}$ given in Definition 14, the global average of the local models follows the following dynamics:

$$\begin{aligned} \bar{\mathbf{w}}^{(t_{k+1})} &= \bar{\mathbf{w}}^{(t_k)} - \eta_k \sum_{\ell=t_k}^{t_{k+1}-1} \sum_{c=1}^N \varrho_c \frac{1}{s_c} \sum_{j \in \mathcal{S}_c} \left(\nabla F_j(\mathbf{w}_j^{(\ell)}) - \mathbf{n}_j^{(\ell)} \right) \\ &+ \sum_{\ell \in \mathcal{T}_{k,c}^L} \sum_{c=1}^N \varrho_c \bar{\mathbf{n}}_{c,Loc}^{(\ell)} + \bar{\mathbf{n}}_{Glob}^{(t_{k+1})}, \end{aligned} \quad (39)$$

where $\mathbf{n}_j^{(\ell)} = \widehat{\mathbf{g}}_j^{(\ell)} - \nabla F_j(\mathbf{w}_j^{(\ell)})$. On the other hand, the β -smoothness of the global function F implies

$$F(\bar{\mathbf{w}}^{(t_{k+1})}) \leq F(\bar{\mathbf{w}}^{(t_k)}) + \nabla F(\bar{\mathbf{w}}^{(t_k)})^\top (\bar{\mathbf{w}}^{(t_{k+1})} - \bar{\mathbf{w}}^{(t_k)}) + \frac{\beta}{2} \|\bar{\mathbf{w}}^{(t_{k+1})} - \bar{\mathbf{w}}^{(t_k)}\|^2. \quad (40)$$

Replacing the result of (39) in the above inequality, taking the expectation on the both hand sides, and using the fact that $\mathbb{E}[\mathbf{n}_j^{(\ell)}] = \mathbf{0}$ and $\mathbb{E}[\bar{\mathbf{n}}_{Glob}^{(t_{k+1})}] = \mathbf{0}$ yields:

$$\begin{aligned} \mathbb{E} \left[F(\bar{\mathbf{w}}^{(t_{k+1})}) - F(\bar{\mathbf{w}}^{(t_k)}) \right] &\leq - \underbrace{\sum_{\ell=t_k}^{t_{k+1}-1} \mathbb{E} \left[\eta_k \nabla F(\bar{\mathbf{w}}^{(t_k)})^\top \sum_{c=1}^N \varrho_c \sum_{j \in \mathcal{S}_c} \rho_{j,c} \nabla F_j(\mathbf{w}_j^{(\ell)}) \right]}_{(a)} \\ &+ \underbrace{\frac{\eta_k^2 \beta}{2} \mathbb{E} \left[\left\| \sum_{\ell=t_k}^{t_{k+1}-1} \sum_{c=1}^N \varrho_c \sum_{j \in \mathcal{S}_c} \rho_{j,c} \nabla F_j(\mathbf{w}_j^{(\ell)}) \right\|^2 \right]}_{(b_1)} + \underbrace{\frac{\eta_k^2 \beta}{2} \mathbb{E} \left[\left\| \sum_{\ell=t_k}^{t_{k+1}-1} \sum_{c=1}^N \varrho_c \sum_{j \in \mathcal{S}_c} \rho_{j,c} \mathbf{n}_j^{(\ell)} \right\|^2 \right]}_{(b_2)} \\ &+ \underbrace{\frac{\beta}{2} \mathbb{E} \left[\left\| \bar{\mathbf{n}}_{Glob}^{(t_{k+1})} \right\|^2 \right]}_{(c_1)} + \underbrace{\frac{\beta}{2} \mathbb{E} \left[\left\| \sum_{\ell \in \mathcal{T}_{k,c}^L} \sum_{c=1}^N \varrho_c \bar{\mathbf{n}}_{c,Loc}^{(\ell)} \right\|^2 \right]}_{(c_2)}. \end{aligned} \quad (41)$$

To bound (a), we apply Lemma C.3 (see Appendix C) to get

$$\begin{aligned} & -\eta_k \sum_{\ell=t_k}^{t_{k+1}-1} \left[\nabla F(\bar{\mathbf{w}}^{(t_k)})^\top \sum_{c=1}^N \varrho_c \sum_{j \in \mathcal{S}_c} \rho_{j,c} \nabla F_j(\mathbf{w}_j^{(\ell)}) \right] \leq -\frac{\eta_k \tau}{2} \left\| \nabla F(\bar{\mathbf{w}}^{(t_k)}) \right\|^2 \\ & -\frac{\eta_k}{2} \sum_{\ell=t_k}^{t_{k+1}-1} \left\| \sum_{c=1}^N \varrho_c \sum_{j \in \mathcal{S}_c} \rho_{j,c} \nabla F_j(\mathbf{w}_j^{(\ell)}) \right\|^2 + \frac{\eta_k \beta^2}{2} \sum_{\ell=t_k}^{t_{k+1}-1} \sum_{c=1}^N \varrho_c \sum_{j \in \mathcal{S}_c} \rho_{j,c} \left\| \bar{\mathbf{w}}^{(\ell)} - \mathbf{w}_j^{(\ell)} \right\|^2 + \frac{\eta_k^3 \beta^2 \tau^2 G^2}{2}, \end{aligned} \quad (42)$$

To bound (b₁) and (b₂), we use the Cauchy-Schwartz inequality (i.e., $\| \sum_{n=1}^N \mathbf{a}_n \|^2 \leq N \sum_{n=1}^N \| \mathbf{a}_n \|^2$ holds for any real-values set of vectors $\{ \mathbf{a}_n \}_{n=1}^N$) to get

$$\left\| \sum_{\ell=t_k}^{t_{k+1}-1} \sum_{c=1}^N \varrho_c \sum_{j \in \mathcal{S}_c} \rho_{j,c} \nabla F_j(\mathbf{w}_j^{(\ell)}) \right\|^2 \leq \tau \sum_{\ell=t_k}^{t_{k+1}-1} \left\| \sum_{c=1}^N \varrho_c \sum_{j \in \mathcal{S}_c} \rho_{j,c} \nabla F_j(\mathbf{w}_j^{(\ell)}) \right\|^2. \quad (43)$$

and

$$\left\| \sum_{\ell=t_k}^{t_{k+1}-1} \sum_{c=1}^N \varrho_c \sum_{j \in \mathcal{S}_c} \rho_{j,c} \mathbf{n}_j^{(\ell)} \right\|^2 \leq \tau \sum_{\ell=t_k}^{t_{k+1}-1} \left\| \sum_{c=1}^N \varrho_c \sum_{j \in \mathcal{S}_c} \rho_{j,c} \mathbf{n}_j^{(\ell)} \right\|^2 \leq \tau \sum_{\ell=t_k}^{t_{k+1}-1} \sum_{c=1}^N \varrho_c \sum_{j \in \mathcal{S}_c} \rho_{j,c} \left\| \mathbf{n}_j^{(\ell)} \right\|^2. \quad (44)$$

To bound (c₁), we first show that

$$\bar{\mathbf{n}}_{Glob}^{(t)} = \sum_{c=1}^N \varrho_c \bar{\mathbf{n}}_{c,Glob}^{(t)}. \quad (45)$$

Since $\bar{\mathbf{n}}_{c,Glob}^{(t)}$ are i.i.d. random variables for $c = 1, 2, \dots, N$, we get

$$\mathbb{E}[\| \bar{\mathbf{n}}_{Glob}^{(t)} \|^2] = \mathbb{E}[\left\| \sum_{c=1}^N \varrho_c \bar{\mathbf{n}}_{c,Glob}^{(t)} \right\|^2] = \sum_{c=1}^N \varrho_c^2 \underbrace{\mathbb{E}[\| \bar{\mathbf{n}}_{c,Glob}^{(t)} \|^2]}_{(d)}. \quad (46)$$

To bound (d), we apply the law of total expectation and get

$$\begin{aligned} & \mathbb{E}[\| \bar{\mathbf{n}}_{c,Glob}^{(t)} \|^2] \\ & = p_c \cdot \mathbb{E}[\| \tilde{\mathbf{n}}_{c,Glob}^{(t)} \|^2 | \tilde{\mathbf{n}}_{c,Glob}^{(t)} \sim \mathcal{N}(0, \bar{\sigma}_{Glob}^2)] + (1-p_c) \cdot \mathbb{E}[\left\| \sum_{j \in \mathcal{S}_c} \rho_{j,c} \mathbf{n}_{j,Glob}^{(t)} \right\|^2 | \mathbf{n}_{j,Glob}^{(t)} \sim \mathcal{N}(0, \sigma_{Glob}^2)] \\ & \stackrel{(i)}{=} \underbrace{p_c \mathbb{E}[\| \tilde{\mathbf{n}}_{c,Glob}^{(t)} \|^2 | \tilde{\mathbf{n}}_{c,Glob}^{(t)} \sim \mathcal{N}(0, \bar{\sigma}_{Glob}^2)]}_{(d_1)} + (1-p_c) \sum_{j \in \mathcal{S}_c} \rho_{j,c}^2 \underbrace{\mathbb{E}[\| \mathbf{n}_{j,Glob}^{(t)} \|^2 | \mathbf{n}_{j,Glob}^{(t)} \sim \mathcal{N}(0, \sigma_{Glob}^2)]}_{(d_2)}. \end{aligned} \quad (47)$$

where (i) comes from the fact that $\mathbf{n}_{j,Glob}^{(t)}$ are i.i.d. random variables for $j \in \mathcal{S}_c$ and $\mathbb{E}[\mathbf{n}_{j,Glob}^{(t)}] = 0, \forall j \in \mathcal{S}_c$. To bound (d₁) in the above inequality, we show that

$$\mathbb{E}[\| \tilde{\mathbf{n}}_{c,Glob}^{(t)} \|^2 | \tilde{\mathbf{n}}_{c,Glob}^{(t)} \sim \mathcal{N}(0, \bar{\sigma}_{Glob}^2)] = \mathbb{E} \left[\sum_{n=0}^{M-1} (\bar{n}_{\{c,n\},Glob}^{(t)})^2 \right] = \sum_{n=0}^{M-1} \mathbb{E} \left[(\bar{n}_{\{c,n\},Glob}^{(t)})^2 \right] = M \bar{\sigma}_{Glob}^2, \quad (48)$$

where $\bar{\mathbf{n}}_{c,Glob}^{(t)} = (\bar{n}_{\{c,0\},Glob}^{(t)}, \bar{n}_{\{c,1\},Glob}^{(t)}, \dots, \bar{n}_{\{c,M-1\},Glob}^{(t)})$. Similarly, to bound (d₂), we show that

$$\mathbb{E}[\| \mathbf{n}_{j,Glob}^{(t)} \|^2 | \mathbf{n}_{j,Glob}^{(t)} \sim \mathcal{N}(0, \sigma_{Glob}^2)] = \mathbb{E} \left[\sum_{n=0}^{M-1} (n_{\{j,n\},Glob}^{(t)})^2 \right] = \sum_{n=0}^{M-1} \mathbb{E} \left[(n_{\{j,n\},Glob}^{(t)})^2 \right] = M \sigma_{Glob}^2, \quad (49)$$

where $\mathbf{n}_{j,Glob}^{(t)} = (n_{\{j,0\},Glob}^{(t)}, n_{\{j,1\},Glob}^{(t)}, \dots, n_{\{j,M-1\},Glob}^{(t)})$. Replacing (48) and (49) into (47) gives us

$$\mathbb{E}[\| \bar{\mathbf{n}}_{c,Glob}^{(t)} \|^2] = M \left(p_c \bar{\sigma}_{Glob}^2 + (1-p_c) \sigma_{Glob}^2 \sum_{j \in \mathcal{S}_c} \rho_{j,c}^2 \right). \quad (50)$$

Utilize the result above in (46) yields

$$\mathbb{E}[\| \bar{\mathbf{n}}_{Glob}^{(t)} \|^2] = M \sum_{c=1}^N \varrho_c^2 \left(p_c \bar{\sigma}_{Glob}^2 + (1-p_c) \sigma_{Glob}^2 \sum_{j \in \mathcal{S}_c} \rho_{j,c}^2 \right). \quad (51)$$

To bound (c_2) , we first apply the Cauchy-Schwartz inequality as follows:

$$\mathbb{E} \left[\left\| \sum_{\ell \in \mathcal{I}_{k,c}^L} \sum_{c=1}^N \varrho_c \bar{\mathbf{n}}_{c,Loc}^{(\ell)} \right\|^2 \right] \leq K_\ell \sum_{\ell \in \mathcal{I}_{k,c}^L} \mathbb{E} \left[\left\| \sum_{c=1}^N \varrho_c \bar{\mathbf{n}}_{c,Loc}^{(\ell)} \right\|^2 \right]. \quad (52)$$

Applying the result from (101) in Lemma C.2, we get

$$\begin{aligned} \mathbb{E} \left[\left\| \sum_{\ell \in \mathcal{I}_{k,c}^L} \sum_{c=1}^N \varrho_c \bar{\mathbf{n}}_{c,Loc}^{(\ell)} \right\|^2 \right] &\leq K_\ell M \sum_{\ell=t_k}^{t_{k+1}-1} \sum_{d=1}^N \varrho_d^2 \left(p_d \bar{\sigma}_{Loc}^2 + (1-p_d) \sigma_{Loc}^2 \sum_{j \in \mathcal{S}_d} \rho_{j,d}^2 \right) \\ &= K_\ell^2 M \sum_{d=1}^N \varrho_d^2 \left(p_d \bar{\sigma}_{Loc}^2 + (1-p_d) \sigma_{Loc}^2 \sum_{j \in \mathcal{S}_d} \rho_{j,d}^2 \right). \end{aligned} \quad (53)$$

Substituting (42), (43) (44), and (53) into (41), using the facts $\mathbb{E}[\|\mathbf{n}_j^{(\ell)}\|_2^2] \leq \sigma^2$, and Cauchy-Schwartz inequality yields

$$\begin{aligned} \mathbb{E} \left[F(\bar{\mathbf{w}}^{(t_{k+1})}) - F(\bar{\mathbf{w}}^{(t_k)}) \right] &\leq -\frac{\eta_k \tau}{2} \mathbb{E}[\|\nabla F(\bar{\mathbf{w}}^{(t_k)})\|^2] + \frac{\eta_k \beta^2}{2} \sum_{\ell=t_k}^{t_{k+1}-1} \left[Z_1^{(\ell)} + Z_2^{(\ell)} \right] \\ &+ \frac{\eta_k^2 \beta \tau (G^2 + \tau \sigma^2)}{2} + \frac{\beta M}{2} \sum_{c=1}^N \varrho_c^2 \left(p_c \bar{\sigma}_{Glob}^2 + (1-p_c) \sigma_{Glob}^2 \sum_{j \in \mathcal{S}_c} \rho_{j,c}^2 \right) \\ &+ \frac{\beta K_\ell^2 M}{2} \sum_{d=1}^N \varrho_d^2 \left(p_d \bar{\sigma}_{Loc}^2 + (1-p_d) \sigma_{Loc}^2 \sum_{j \in \mathcal{S}_d} \rho_{j,d}^2 \right). \end{aligned} \quad (54)$$

Applying Proposition 3.1&4.2 into the inequality above yields

$$\begin{aligned} \mathbb{E} \left[F(\bar{\mathbf{w}}^{(t_{k+1})}) - F(\bar{\mathbf{w}}^{(t_k)}) \right] &\leq -\frac{\eta_k \tau}{2} \mathbb{E}[\|\nabla F(\bar{\mathbf{w}}^{(t_k)})\|^2] + \frac{\eta_k^2 \beta^2}{2} \tau^2 \left(B_1^2 + B_2^2 \right) + \frac{\eta_k^2 \beta \tau (G^2 + \tau \sigma^2)}{2} \\ &+ \frac{\beta K_\ell^3 K_g M q^2 \log(1/\delta)}{2N^2 \varepsilon^2} \sum_{d=1}^N \varrho_d^2 \left(p_d c_2^2 \Delta_{Edge,Loc}^2 + (1-p_d) \frac{v_2^2}{s_c} \Delta_{Device,Loc}^2 \right) \\ &+ \frac{\beta M q^2 K_g \log(1/\delta)}{2N^2 \varepsilon^2} \sum_{c=1}^N \left(p_c c_2^2 \Delta_{Edge,Glob}^2 + (1-p_c) \frac{v_2^2}{s_c} \Delta_{Device,Glob}^2 \right). \end{aligned} \quad (55)$$

Replacing the bound on $\Delta_{Edge,Glob}$ and $\Delta_{Device,Glob}$ from Lemma C.1 into (55) and using the fact that $\eta_k \leq \frac{1}{\max\{\tau, K_g\} \beta}$ gives us

$$\begin{aligned} \frac{\eta_k \tau}{2} \mathbb{E}[\|\nabla F(\bar{\mathbf{w}}^{(t_k)})\|^2] &\leq \mathbb{E} \left[F(\bar{\mathbf{w}}^{(t_k)}) - F(\bar{\mathbf{w}}^{(t_{k+1})}) \right] + \frac{\eta_k^2 \beta \tau}{2} \left[\beta \tau \left(B_1^2 + B_2^2 \right) + G^2 + \tau \sigma^2 \right] \\ &+ \eta_k (K_\ell^3 + 1) \frac{2\tau^2 M q^2 G^2 \log(1/\delta)}{N^2 \varepsilon^2} \sum_{c=1}^N \left(p_c \frac{c_2^2}{s_c} + (1-p_c) \frac{v_2^2}{s_c} \right). \end{aligned} \quad (56)$$

Dividing both hand sides by $\frac{\eta_k \tau}{2}$ and averaging across global aggregations yields

$$\begin{aligned} \frac{1}{K_g} \sum_{k=0}^{K_g-1} \mathbb{E}[\|\nabla F(\bar{\mathbf{w}}^{(t_k)})\|^2] &\leq \frac{1}{K_g} \sum_{k=0}^{K_g-1} \left[\frac{2}{\eta_k \tau} \mathbb{E} \left[F(\bar{\mathbf{w}}^{(t_k)}) - F(\bar{\mathbf{w}}^{(t_{k+1})}) \right] \right] \\ &+ \frac{1}{K_g} \sum_{k=0}^{K_g-1} \left[\eta_k \beta \left[\beta \tau \left(B_1^2 + B_2^2 \right) + G^2 + \tau \sigma^2 \right] \right] + \frac{4\tau (K_\ell^3 + 1) M q^2 G^2 \log(1/\delta)}{N^2 \varepsilon^2} \sum_{c=1}^N \left(p_c \frac{c_2^2}{s_c} + (1-p_c) \frac{v_2^2}{s_c} \right) \\ &\leq 2\gamma \frac{F(\bar{\mathbf{w}}^{(0)}) - F(\mathbf{w}^*)}{\tau \sqrt{K_g + 1}} + \frac{\beta \gamma}{\sqrt{K_g + 1}} \left[\beta \tau \left(B_1^2 + B_2^2 \right) + G^2 + \tau \sigma^2 \right] \\ &+ \frac{4\tau (K_\ell^3 + 1) M q^2 G^2 \log(1/\delta)}{N^2 \varepsilon^2} \sum_{c=1}^N \left(p_c \frac{c_2^2}{s_c} + (1-p_c) \frac{v_2^2}{s_c} \right). \end{aligned} \quad (57)$$

□

B PROOF OF PROPOSITION B.1

PROPOSITION B.1. For $t \in \mathcal{T}_k \setminus \{t_{k+1}\}$, under Assumptions 1 and 2, if $\eta_k \leq \frac{1}{\max\{\tau, K_g\}\beta}$, using DP-HFL for ML model training, the model dispersion can be bounded as

$$Z_1^{(t)} \leq \eta_k \tau B_1^2, \quad (58)$$

and

$$Z_2^{(t)} \leq \eta_k \tau B_2^2. \quad (59)$$

where

$$B_1 = \left((1 + 2\eta_0\beta)^{\tau-1} + 1 \right)^2 \sum_{c=1}^N \varrho_c \left(2\sigma + \zeta_c \right)^2, \quad (60)$$

$$B_2 = (1 + \eta_k\beta)^{2(\tau-1)} \sum_{c=1}^N \varrho_c \Phi_c^2, \quad (61)$$

and

$$\begin{aligned} \Phi_c = & \left[\frac{2Cq\sqrt{M\log(1/\delta)}}{\varepsilon} \left(\sqrt{\sum_{c=1}^N \left(p_c \frac{c_2^2}{N^2 s_c^2} + (1-p_c) \frac{v_2^2}{N^2 s_c} \right)} + \sqrt{p_c \frac{c_2^2}{s_c^2} + (1-p_c) \frac{v_2^2}{s_c}} \right) \right. \\ & \left. + 2\beta\epsilon_k + 2\sigma + \zeta \right] \left((1 + \eta_0(\beta - \mu))^{\tau-1} + 1 \right) + \beta(\epsilon_{c,k} + \epsilon_k) + 2\sigma + \zeta. \end{aligned} \quad (62)$$

PROOF. B.1 Obtaining bound of $Z_1^{(t)}$.

Applying the one-step behavior of $\sqrt{\mathbb{E}[\|\mathbf{e}_i^{(t+1)}\|^2]}$ from (85) in Lemma C.2, we get

$$\sqrt{\mathbb{E}[\|\mathbf{e}_i^{(t+1)}\|^2]} \leq (1 - \Theta_c^{(t+1)}) \left[(1 + \eta_k\beta) \sqrt{\mathbb{E}[\|\mathbf{e}_i^{(t)}\|^2]} + \underbrace{\eta_k\beta \sum_{j \in \mathcal{S}_c} \rho_{j,c} \sqrt{\mathbb{E}[\|\mathbf{e}_j^{(t)}\|^2]}}_{(a)} + \eta_k(2\sigma + \zeta_c) \right]. \quad (63)$$

We first bound (a) by taking the weighted sum $\sum_{i \in \mathcal{S}_c} \rho_{i,c}$ on the both hand sides of (63) and obtain

$$\begin{aligned} \sum_{j \in \mathcal{S}_c} \rho_{j,c} \sqrt{\mathbb{E}[\|\mathbf{e}_j^{(t+1)}\|^2]} & \leq (1 - \Theta_c^{(t+1)}) \left[(1 + 2\eta_k\beta) \sum_{j \in \mathcal{S}_c} \rho_{j,c} \sqrt{\mathbb{E}[\|\mathbf{e}_j^{(t)}\|^2]} + \eta_k(2\sigma + \zeta_c) \right] \\ & \leq (1 + 2\eta_k\beta) \sum_{j \in \mathcal{S}_c} \rho_{j,c} \sqrt{\mathbb{E}[\|\mathbf{e}_j^{(t)}\|^2]} + \eta_k(2\sigma + \zeta_c). \end{aligned} \quad (64)$$

Recursively expanding across the interval $t \in \mathcal{T}_k$, the above inequality gives us

$$\begin{aligned} \sum_{j \in \mathcal{S}_c} \rho_{j,c} \sqrt{\mathbb{E}[\|\mathbf{e}_j^{(t)}\|^2]} & \leq \eta_k(2\sigma + \zeta_c) \sum_{\ell=t_{k-1}}^{t-1} (1 + 2\eta_k\beta)^{t-\ell-1} \\ & = \eta_k(2\sigma + \zeta_c) \frac{(1 + 2\eta_k\beta)^{t-t_k} - 1}{(1 + 2\eta_k\beta) - 1} \\ & \stackrel{(i)}{\leq} \eta_k(2\sigma + \zeta_c) \frac{2\eta_k\beta\tau(1 + 2\eta_k\beta)^{\tau-1}}{2\eta_k\beta} \\ & \leq \eta_k(2\sigma + \zeta_c)\tau(1 + 2\eta_k\beta)^{\tau-1}. \end{aligned} \quad (65)$$

where (i) utilizes Fact 2. Replacing the bound on (a) into (63) gives us

$$\begin{aligned} \sqrt{\mathbb{E}[\|\mathbf{e}_i^{(t+1)}\|^2]} & \leq (1 - \Theta_c^{(t+1)}) \left[(1 + \eta_k\beta) \sqrt{\mathbb{E}[\|\mathbf{e}_i^{(t)}\|^2]} + \eta_k^2\beta\tau(2\sigma + \zeta_c)(1 + 2\eta_k\beta)^{\tau-1} + \eta_k(2\sigma + \zeta_c) \right] \\ & \leq (1 + \eta_k\beta) \sqrt{\mathbb{E}[\|\mathbf{e}_i^{(t)}\|^2]} + \eta_k \left[(2\sigma + \zeta_c) \left((1 + 2\eta_k\beta)^{\tau-1} + 1 \right) \right]. \end{aligned} \quad (66)$$

Recursively expanding the above inequality across the interval $t \in \mathcal{T}_k$ results in

$$\begin{aligned}
\sqrt{\mathbb{E}[\|\mathbf{e}_i^{(t)}\|^2]} &\leq \eta_k \left[(2\sigma + \zeta_c) \left((1 + 2\eta_k\beta)^{\tau-1} + 1 \right) \right] \sum_{\ell=t_k}^{t-1} (1 + \eta_k\beta)^{t-\ell-1} \prod_{m=\ell+1}^t (1 - \Theta_c^{(m)}) \\
&= \eta_k \left[(2\sigma + \zeta_c) \left((1 + 2\eta_k\beta)^{\tau-1} + 1 \right) \right] \frac{(1 + \eta_k\beta\mu)^{t-t_k} - 1}{(1 + \eta_k\beta) - 1} \\
&\leq \eta_k \left[(2\sigma + \zeta_c) \left((1 + 2\eta_k\beta)^{\tau-1} + 1 \right) \right] \frac{\eta_k\beta\tau(1 + \eta_k\beta)^{\tau-1}}{\eta_k\beta} \\
&\leq \eta_k\tau \left[(2\sigma + \zeta_c) \left((1 + 2\eta_k\beta)^{\tau-1} + 1 \right) \right].
\end{aligned} \tag{67}$$

Taking square of both hand sides followed by taking the weighted sum $\sum_{c=1}^N \varrho_c \sum_{j \in \mathcal{S}_c} \rho_{j,c}$ gives us

$$Z_1^{(t)} \leq \eta_k^2 \tau^2 B_1^2 \leq \eta_k \tau B_1^2 \tag{68}$$

B.2 Obtaining bound of $Z_2^{(t)}$.

Applying the one-step behavior of $\sqrt{\mathbb{E}[\|\bar{\mathbf{w}}_c^{(t+1)} - \bar{\mathbf{w}}^{(t+1)}\|^2]}$ from (86) in Lemma C.2, we get

$$\begin{aligned}
\sqrt{\mathbb{E}[\|\bar{\mathbf{w}}_c^{(t+1)} - \bar{\mathbf{w}}^{(t+1)}\|^2]} &\leq (1 + \eta_k\beta) \sqrt{\mathbb{E}[\|\bar{\mathbf{w}}_c^{(t)} - \bar{\mathbf{w}}^{(t)}\|^2]} + \underbrace{\eta_k\beta \sum_{d=1}^N \varrho_d \sqrt{\mathbb{E}[\|\bar{\mathbf{w}}_d^{(t)} - \bar{\mathbf{w}}^{(t)}\|^2]}}_{(b)} \\
&+ \eta_k\beta\epsilon_{c,k} + \eta_k\beta\epsilon_k + \eta_k(2\sigma + \zeta) + \sqrt{M \sum_{d=1}^N \varrho_d^2 \Theta_d^{(t+1)} (p_d \bar{\sigma}_{Loc}^2 + (1 - p_d) \sigma_{Loc}^2 \sum_{j \in \mathcal{S}_d} \rho_{j,d}^2)} \\
&+ \Theta_c^{(t+1)} \sqrt{M (p_c \bar{\sigma}_{Loc}^2 + (1 - p_c) \sigma_{Loc}^2 \sum_{j \in \mathcal{S}_c} \rho_{j,c}^2)}.
\end{aligned} \tag{69}$$

We first bound (b) by taking the weighted sum $\sum_{c=1}^N \varrho_c$ on the both hand sides of (69) and get

$$\begin{aligned}
\sum_{c=1}^N \varrho_c \sqrt{\mathbb{E}[\|\bar{\mathbf{w}}_c^{(t+1)} - \bar{\mathbf{w}}^{(t+1)}\|^2]} &\leq (1 + 2\eta_k\beta) \sum_{c=1}^N \varrho_c \sqrt{\mathbb{E}[\|\bar{\mathbf{w}}_c^{(t)} - \bar{\mathbf{w}}^{(t)}\|^2]} \\
&+ \eta_k(2\beta\epsilon_k + 2\sigma + \zeta) + \sqrt{M \sum_{d=1}^N \varrho_d^2 \Theta_d^{(t+1)} (p_d \bar{\sigma}_{Loc}^2 + (1 - p_d) \sigma_{Loc}^2 \sum_{j \in \mathcal{S}_d} \rho_{j,d}^2)} \\
&+ \Theta_c^{(t+1)} \sqrt{M (p_c \bar{\sigma}_{Loc}^2 + (1 - p_c) \sigma_{Loc}^2 \sum_{j \in \mathcal{S}_c} \rho_{j,c}^2)} \\
&\leq (1 + 2\eta_k\beta) \sum_{c=1}^N \varrho_c \sqrt{\mathbb{E}[\|\bar{\mathbf{w}}_c^{(t)} - \bar{\mathbf{w}}^{(t)}\|^2]} + \eta_k(2\beta\epsilon_k + 2\sigma + \zeta) \\
&+ \sqrt{M \sum_{d=1}^N \varrho_d^2 (p_d \bar{\sigma}_{Loc}^2 + (1 - p_d) \sigma_{Loc}^2 \sum_{j \in \mathcal{S}_d} \rho_{j,d}^2)} + \sqrt{M (p_c \bar{\sigma}_{Loc}^2 + (1 - p_c) \sigma_{Loc}^2 \sum_{j \in \mathcal{S}_c} \rho_{j,c}^2)}.
\end{aligned} \tag{70}$$

Recursively expanding across the interval $t \in \mathcal{T}_k$, the above inequality yields

$$\begin{aligned}
&\sum_{c=1}^N \varrho_c \sqrt{\mathbb{E}[\|\bar{\mathbf{w}}_c^{(t)} - \bar{\mathbf{w}}^{(t)}\|^2]} \\
&\leq \left(\eta_k(2\beta\epsilon_k + 2\sigma + \zeta) + \sqrt{M \sum_{d=1}^N \varrho_d^2 (p_d \bar{\sigma}_{Loc}^2 + (1 - p_d) \sigma_{Loc}^2 \sum_{j \in \mathcal{S}_d} \rho_{j,d}^2)} \right) \\
&+ \sqrt{M (p_c \bar{\sigma}_{Loc}^2 + (1 - p_c) \sigma_{Loc}^2 \sum_{j \in \mathcal{S}_c} \rho_{j,c}^2)} \sum_{\ell=t_k}^{t-1} (1 + 2\eta_k\beta)^{t-\ell-1}
\end{aligned}$$

$$\begin{aligned}
&= \left(\eta_k(2\beta\epsilon_k + 2\sigma + \zeta) + \sqrt{M \sum_{d=1}^N \varrho_d^2 \left(p_d \bar{\sigma}_{Loc}^2 + (1-p_d) \sigma_{Loc}^2 \sum_{j \in \mathcal{S}_d} \rho_{j,d}^2 \right)} \right) \\
&+ \sqrt{M \left(p_c \bar{\sigma}_{Loc}^2 + (1-p_c) \sigma_{Loc}^2 \sum_{j \in \mathcal{S}_c} \rho_{j,c}^2 \right)} \frac{(1+2\eta_k\beta)^{t-t_k} - 1}{(1+2\eta_k\beta) - 1} \\
&\stackrel{(iii)}{\leq} \left(\eta_k(2\beta\epsilon_k + 2\sigma + \zeta) + \sqrt{M \sum_{d=1}^N \varrho_d^2 \left(p_d \bar{\sigma}_{Loc}^2 + (1-p_d) \sigma_{Loc}^2 \sum_{j \in \mathcal{S}_d} \rho_{j,d}^2 \right)} \right) \\
&+ \sqrt{M \left(p_c \bar{\sigma}_{Loc}^2 + (1-p_c) \sigma_{Loc}^2 \sum_{j \in \mathcal{S}_c} \rho_{j,c}^2 \right)} \frac{2\eta_k\beta\tau(1+2\eta_k\beta)^{t-t_k-1}}{2\eta_k\beta} \\
&\leq \tau \left(\eta_k(2\beta\epsilon_k + 2\sigma + \zeta) + \sqrt{M \sum_{d=1}^N \varrho_d^2 \left(p_d \bar{\sigma}_{Loc}^2 + (1-p_d) \sigma_{Loc}^2 \sum_{j \in \mathcal{S}_d} \rho_{j,d}^2 \right)} \right) \\
&+ \sqrt{M \left(p_c \bar{\sigma}_{Loc}^2 + (1-p_c) \sigma_{Loc}^2 \sum_{j \in \mathcal{S}_c} \rho_{j,c}^2 \right)} (1+2\eta_k\beta)^{\tau-1}, \tag{71}
\end{aligned}$$

where (iii) is resulted from Fact. 2. Replacing the bound on (b) above into (69) yields

$$\begin{aligned}
&\sqrt{\mathbb{E}[\|\bar{\mathbf{w}}_c^{(t+1)} - \bar{\mathbf{w}}^{(t+1)}\|^2]} \leq (1-\eta_k\mu) \sqrt{\mathbb{E}[\|\bar{\mathbf{w}}_c^{(t)} - \bar{\mathbf{w}}^{(t)}\|^2]} \\
&+ \eta_k\beta\tau \left(\eta_k(2\beta\epsilon_k + 2\sigma + \zeta) + \sqrt{M \sum_{d=1}^N \varrho_d^2 \left(p_d \bar{\sigma}_{Loc}^2 + (1-p_d) \sigma_{Loc}^2 \sum_{j \in \mathcal{S}_d} \rho_{j,d}^2 \right)} \right) \\
&+ \sqrt{M \left(p_c \bar{\sigma}_{Loc}^2 + (1-p_c) \sigma_{Loc}^2 \sum_{j \in \mathcal{S}_c} \rho_{j,c}^2 \right)} (1+2\eta_k\beta)^{\tau-1} + \eta_k(\beta(\epsilon_{c,k} + \epsilon_k) + 2\sigma + \zeta) \\
&+ \sqrt{M \sum_{d=1}^N \varrho_d^2 \Theta_d^{(t+1)} \left(p_d \bar{\sigma}_{Loc}^2 + (1-p_d) \sigma_{Loc}^2 \sum_{j \in \mathcal{S}_d} \rho_{j,d}^2 \right)} \\
&+ \Theta_c^{(t+1)} \sqrt{M \left(p_c \bar{\sigma}_{Loc}^2 + (1-p_c) \sigma_{Loc}^2 \sum_{j \in \mathcal{S}_c} \rho_{j,c}^2 \right)} \\
&\leq (1-\eta_k\mu) \sqrt{\mathbb{E}[\|\bar{\mathbf{w}}_c^{(t)} - \bar{\mathbf{w}}^{(t)}\|^2]} \\
&+ \eta_k\beta\tau \left(\eta_k(2\beta\epsilon_k + 2\sigma + \zeta) + \sqrt{M \sum_{d=1}^N \varrho_d^2 \left(p_d \bar{\sigma}_{Loc}^2 + (1-p_d) \sigma_{Loc}^2 \sum_{j \in \mathcal{S}_d} \rho_{j,d}^2 \right)} \right) \\
&+ \sqrt{M \left(p_c \bar{\sigma}_{Loc}^2 + (1-p_c) \sigma_{Loc}^2 \sum_{j \in \mathcal{S}_c} \rho_{j,c}^2 \right)} (1+2\eta_k\beta)^{\tau-1} + \eta_k(\beta(\epsilon_{c,k} + \epsilon_k) + 2\sigma + \zeta) \\
&+ \sqrt{M \sum_{d=1}^N \varrho_d^2 \left(p_d \bar{\sigma}_{Loc}^2 + (1-p_d) \sigma_{Loc}^2 \sum_{j \in \mathcal{S}_d} \rho_{j,d}^2 \right)} + \sqrt{M \left(p_c \bar{\sigma}_{Loc}^2 + (1-p_c) \sigma_{Loc}^2 \sum_{j \in \mathcal{S}_c} \rho_{j,c}^2 \right)}. \tag{72}
\end{aligned}$$

Apply Proposition 3.1 and Lemma C.1 into the above inequality yields

$$\begin{aligned}
&\sqrt{\mathbb{E}[\|\bar{\mathbf{w}}_c^{(t+1)} - \bar{\mathbf{w}}^{(t+1)}\|^2]} \leq (1+\eta_k\beta) \sqrt{\mathbb{E}[\|\bar{\mathbf{w}}_c^{(t)} - \bar{\mathbf{w}}^{(t)}\|^2]} \\
&+ \eta_k\beta\tau \left[\frac{2Cq\sqrt{MK_\ell K_g \log(1/\delta)}}{\varepsilon} \left(\sqrt{\sum_{d=1}^N \left(p_d \frac{c_2^2}{N^2 s_d^2} + (1-p_d) \frac{v_2^2}{N^2 s_d} \right)} + \sqrt{p_c \frac{c_2^2}{s_c^2} + (1-p_c) \frac{v_2^2}{s_c}} \right) \right. \\
&\left. + 2\beta\epsilon_k + 2\sigma + \zeta \right] (1+2\eta_k\beta)^{\tau-1} + \eta_k(\beta(\epsilon_{c,k} + \epsilon_k) + 2\sigma + \zeta)
\end{aligned}$$

$$+ \eta_k^2 \frac{2Cq\sqrt{MK_\ell K_g \log(1/\delta)}}{\varepsilon} \left(\sqrt{\sum_{d=1}^N \left(p_d \frac{c_2^2}{N^2 s_d^2} + (1-p_d) \frac{v_2^2}{N^2 s_d} \right)} + \sqrt{p_c \frac{c_2^2}{s_c^2} + (1-p_c) \frac{v_2^2}{s_c}} \right). \quad (73)$$

Using the fact that $\eta_k \leq \frac{1}{\max\{\tau, K_g\}\beta}$ on the above inequality, we obtain

$$\begin{aligned} \sqrt{\mathbb{E}[\|\bar{\mathbf{w}}_c^{(t+1)} - \bar{\mathbf{w}}^{(t+1)}\|^2]} &\leq (1 + \eta_k \beta) \sqrt{\mathbb{E}[\|\bar{\mathbf{w}}_c^{(t)} - \bar{\mathbf{w}}^{(t)}\|^2]} \\ &+ \eta_k \left[\frac{2Cq\sqrt{M \log(1/\delta)}}{\varepsilon} \left(\sqrt{\sum_{d=1}^N \left(p_d \frac{c_2^2}{N^2 s_d^2} + (1-p_d) \frac{v_2^2}{N^2 s_d} \right)} + \sqrt{p_c \frac{c_2^2}{s_c^2} + (1-p_c) \frac{v_2^2}{s_c}} \right) \right. \\ &\left. + 2\beta\epsilon_k + 2\sigma + \zeta \right] \left((1 + 2\eta_0 \beta)^{\tau-1} + 1 \right) + \eta_k (\beta(\epsilon_{c,k} + \epsilon_k) + 2\sigma + \zeta) \\ &= (1 - \eta_k \mu) \sqrt{\mathbb{E}[\|\bar{\mathbf{w}}_c^{(t)} - \bar{\mathbf{w}}^{(t)}\|^2]} + \eta_k \Phi_c. \end{aligned} \quad (74)$$

Recursively expanding across the interval $t \in \mathcal{T}_k$, the above inequality yields

$$\begin{aligned} \sqrt{\mathbb{E}[\|\bar{\mathbf{w}}_c^{(t)} - \bar{\mathbf{w}}^{(t)}\|^2]} &\leq \eta_k \Phi_c \sum_{\ell=t_k}^{t-1} (1 + \eta_k \beta)^{t-\ell-1} \\ &= \eta_k \Phi_c \frac{(1 + \eta_k \beta)^{t-t_k} - 1}{(1 + \eta_k \beta) - 1} \\ &= \eta_k \Phi_c \frac{\eta_k \beta \tau (1 + \eta_k \beta)^{\tau-1}}{\eta_k \beta} \\ &\leq \eta_k \tau \Phi_c (1 + \eta_k \beta)^{\tau-1}. \end{aligned} \quad (75)$$

Taking square of both hand sides followed by taking the weighted sum $\sum_{c=1}^N \varrho_c$ gives us

$$Z_2^{(t)} \leq \eta_k^2 \tau^2 B_2^2 \leq \eta_k \tau B_2^2. \quad (76)$$

This concludes the proof. \square

C LEMMAS AND AUXILIARY RESULTS

To improve the tractability of the proofs, we provide a set of lemmas in the following, which will be used to obtain the main results of the paper.

LEMMA C.1. *Under Assumption 2, the L_2 -norm sensitivity of the exchanged gradients during local aggregations can be obtained as follows:*

$$\bar{\Delta}_{c,Loc} = \max_{\mathcal{D}, \mathcal{D}'} \left\| \eta_k \sum_{\ell=t'}^t \sum_{j \in \mathcal{S}_c} \rho_{j,c} \widehat{\mathbf{g}}_j^{(\ell)}(\mathcal{D}) - \eta_k \sum_{\ell=t'}^t \sum_{j \in \mathcal{S}_c} \rho_{j,c} \widehat{\mathbf{g}}_j^{(\ell)}(\mathcal{D}') \right\| = 2\eta_k \tau_k G / s_c, \quad (77)$$

and

$$\Delta_{i,Loc} = \max_{\mathcal{D}, \mathcal{D}'} \left\| \eta_k \sum_{\ell=t'}^t \widehat{\mathbf{g}}_i^{(\ell)}(\mathcal{D}) - \eta_k \sum_{\ell=t'}^t \widehat{\mathbf{g}}_i^{(\ell)}(\mathcal{D}') \right\| = 2\eta_k \tau_k G. \quad (78)$$

Similarly, the L_2 -norm sensitivity of the exchanged gradients during global aggregations can be obtained as follows:

$$\bar{\Delta}_{c,Glob} = \max_{\mathcal{D}, \mathcal{D}'} \left\| \eta_k \sum_{\ell=t_k}^{t_{k+1}} \sum_{j \in \mathcal{S}_c} \rho_{j,c} \widehat{\mathbf{g}}_j^{(\ell)}(\mathcal{D}) - \eta_k \sum_{\ell=t_k}^{t_{k+1}} \sum_{j \in \mathcal{S}_c} \rho_{j,c} \widehat{\mathbf{g}}_j^{(\ell)}(\mathcal{D}') \right\| = 2\eta_k \tau_k G / s_c, \quad (79)$$

and

$$\Delta_{i,Glob} = \max_{\mathcal{D}, \mathcal{D}'} \left\| \eta_k \sum_{\ell=t_k}^{t_{k+1}} \widehat{\mathbf{g}}_i^{(\ell)}(\mathcal{D}) - \eta_k \sum_{\ell=t_k}^{t_{k+1}} \widehat{\mathbf{g}}_i^{(\ell)}(\mathcal{D}') \right\| = 2\eta_k \tau_k G. \quad (80)$$

PROOF. Upper bounding $\left\| \eta_k \sum_{\ell=t'}^t \sum_{j \in \mathcal{S}_c} \rho_{j,c} \widehat{\mathbf{g}}_j^{(\ell)}(\mathcal{D}) - \eta_k \sum_{\ell=t'}^t \sum_{j \in \mathcal{S}_c} \rho_{j,c} \widehat{\mathbf{g}}_j^{(\ell)}(\mathcal{D}') \right\|$ yields

$$\begin{aligned} & \left\| \eta_k \sum_{\ell=t'}^t \sum_{j \in \mathcal{S}_c} \rho_{j,c} \widehat{\mathbf{g}}_j^{(\ell)}(\mathcal{D}) - \eta_k \sum_{\ell=t'}^t \sum_{j \in \mathcal{S}_c} \rho_{j,c} \widehat{\mathbf{g}}_j^{(\ell)}(\mathcal{D}') \right\| \\ &= \eta_k \sum_{\ell=t'}^t \left\| \sum_{j \in \mathcal{S}_c} \rho_{j,c} \widehat{\mathbf{g}}_j^{(\ell)}(\mathcal{D}) - \sum_{j \in \mathcal{S}_c} \rho_{j,c} \widehat{\mathbf{g}}_j^{(\ell)}(\mathcal{D}') \right\| \\ &= \eta_k \rho_{j,c} \sum_{\ell=t'}^t \left\| \widehat{\mathbf{g}}_j^{(\ell)}(\mathcal{D}) - \widehat{\mathbf{g}}_j^{(\ell)}(\mathcal{D}') \right\| \leq \eta_k / s_c \sum_{\ell=t'}^t \left(\left\| \widehat{\mathbf{g}}_j^{(\ell)}(\mathcal{D}) \right\| + \left\| \widehat{\mathbf{g}}_j^{(\ell)}(\mathcal{D}') \right\| \right) \\ &\leq \eta_k / s_c \sum_{\ell=t_k}^{t_{k+1}} \left(\left\| \widehat{\mathbf{g}}_j^{(\ell)}(\mathcal{D}) \right\| + \left\| \widehat{\mathbf{g}}_j^{(\ell)}(\mathcal{D}') \right\| \right) \leq \eta_k \tau_k G / s_c. \end{aligned} \quad (81)$$

giving us the result in (77). Similarly, upper bounding $\left\| \eta_k \sum_{\ell=t'}^t \widehat{\mathbf{g}}_i^{(\ell)}(\mathcal{D}) - \eta_k \sum_{\ell=t'}^t \widehat{\mathbf{g}}_i^{(\ell)}(\mathcal{D}') \right\|$, we get

$$\begin{aligned} & \left\| \eta_k \sum_{\ell=t'}^t \widehat{\mathbf{g}}_i^{(\ell)}(\mathcal{D}) - \eta_k \sum_{\ell=t'}^t \widehat{\mathbf{g}}_i^{(\ell)}(\mathcal{D}') \right\| = \eta_k \left\| \sum_{\ell=t'}^t \widehat{\mathbf{g}}_i^{(\ell)}(\mathcal{D}) - \sum_{\ell=t'}^t \widehat{\mathbf{g}}_i^{(\ell)}(\mathcal{D}') \right\| \\ &= \eta_k \sum_{\ell=t'}^t \left\| \widehat{\mathbf{g}}_i^{(\ell)}(\mathcal{D}) - \widehat{\mathbf{g}}_i^{(\ell)}(\mathcal{D}') \right\| \leq \eta_k \sum_{\ell=t'}^t \left(\left\| \widehat{\mathbf{g}}_i^{(\ell)}(\mathcal{D}) \right\| + \left\| \widehat{\mathbf{g}}_i^{(\ell)}(\mathcal{D}') \right\| \right) \\ &\leq \eta_k \sum_{\ell=t_k}^{t_{k+1}} \left(\left\| \widehat{\mathbf{g}}_i^{(\ell)}(\mathcal{D}) \right\| + \left\| \widehat{\mathbf{g}}_i^{(\ell)}(\mathcal{D}') \right\| \right) \leq \eta_k \tau_k G, \end{aligned} \quad (82)$$

giving us the result in (78).

Likewise, upper bounding $\left\| \eta_k \sum_{\ell=t_k}^{t_{k+1}} \sum_{j \in \mathcal{S}_c} \rho_{j,c} \widehat{\mathbf{g}}_j^{(\ell)}(\mathcal{D}) - \eta_k \sum_{\ell=t_k}^{t_{k+1}} \sum_{j \in \mathcal{S}_c} \rho_{j,c} \widehat{\mathbf{g}}_j^{(\ell)}(\mathcal{D}') \right\|$ yields

$$\begin{aligned} \bar{\Delta}_{c,Loc} &= \left\| \eta_k \sum_{\ell=t_k}^{t_{k+1}} \sum_{j \in \mathcal{S}_c} \rho_{j,c} \widehat{\mathbf{g}}_j^{(\ell)}(\mathcal{D}) - \eta_k \sum_{\ell=t_k}^{t_{k+1}} \sum_{j \in \mathcal{S}_c} \rho_{j,c} \widehat{\mathbf{g}}_j^{(\ell)}(\mathcal{D}') \right\| \\ &= \eta_k \sum_{\ell=t_k}^{t_{k+1}} \left\| \sum_{j \in \mathcal{S}_c} \rho_{j,c} \widehat{\mathbf{g}}_j^{(\ell)}(\mathcal{D}) - \sum_{j \in \mathcal{S}_c} \rho_{j,c} \widehat{\mathbf{g}}_j^{(\ell)}(\mathcal{D}') \right\| = \eta_k \rho_{j,c} \sum_{\ell=t_k}^{t_{k+1}} \left\| \widehat{\mathbf{g}}_j^{(\ell)}(\mathcal{D}) - \widehat{\mathbf{g}}_j^{(\ell)}(\mathcal{D}') \right\| \\ &\leq \eta_k / s_c \sum_{\ell=t_k}^{t_{k+1}} \left(\left\| \widehat{\mathbf{g}}_j^{(\ell)}(\mathcal{D}) \right\| + \left\| \widehat{\mathbf{g}}_j^{(\ell)}(\mathcal{D}') \right\| \right) \leq \eta_k \tau_k G / s_c, \end{aligned} \quad (83)$$

giving us the result in (79). Finally, upper bounding $\left\| \eta_k \sum_{\ell=t_k}^{t_{k+1}} \widehat{\mathbf{g}}_i^{(\ell)}(\mathcal{D}) - \eta_k \sum_{\ell=t_k}^{t_{k+1}} \widehat{\mathbf{g}}_i^{(\ell)}(\mathcal{D}') \right\|$, we get

$$\begin{aligned} & \left\| \eta_k \sum_{\ell=t_k}^{t_{k+1}} \widehat{\mathbf{g}}_i^{(\ell)}(\mathcal{D}) - \eta_k \sum_{\ell=t_k}^{t_{k+1}} \widehat{\mathbf{g}}_i^{(\ell)}(\mathcal{D}') \right\| = \eta_k \left\| \sum_{\ell=t_k}^{t_{k+1}} \widehat{\mathbf{g}}_i^{(\ell)}(\mathcal{D}) - \sum_{\ell=t_k}^{t_{k+1}} \widehat{\mathbf{g}}_i^{(\ell)}(\mathcal{D}') \right\| \\ & = \eta_k \sum_{\ell=t_k}^{t_{k+1}} \left\| \widehat{\mathbf{g}}_i^{(\ell)}(\mathcal{D}) - \widehat{\mathbf{g}}_i^{(\ell)}(\mathcal{D}') \right\| \leq \eta_k \sum_{\ell=t_k}^{t_{k+1}} \left(\left\| \widehat{\mathbf{g}}_i^{(\ell)}(\mathcal{D}) \right\| + \left\| \widehat{\mathbf{g}}_i^{(\ell)}(\mathcal{D}') \right\| \right) \leq \eta_k \tau_k G, \end{aligned} \quad (84)$$

giving us the result in (80). \square

LEMMA C.2. For $t \in \mathcal{T}_k \setminus \{t_{k+1}\}$, under Assumptions 1 and 2, using DFL for ML model training, the one-step behavior of $\sqrt{\mathbb{E}[\|\mathbf{e}_j^{(t)}\|^2]}$ and $\sqrt{\mathbb{E}[\|\bar{\mathbf{w}}_c^{(t)} - \bar{\mathbf{w}}^{(t)}\|^2]}$ can be expressed as

$$\sqrt{\mathbb{E}[\|\mathbf{e}_i^{(t+1)}\|^2]} \leq (1 - \Theta_c^{(t+1)}) \left[(1 + \eta_k \beta) \sqrt{\mathbb{E}[\|\mathbf{e}_i^{(t)}\|^2]} + \eta_k \beta \sum_{j \in \mathcal{S}_c} \rho_{j,c} \sqrt{\mathbb{E}[\|\mathbf{e}_j^{(t)}\|^2]} + \eta_k (2\sigma + \zeta_c) \right], \quad (85)$$

and

$$\begin{aligned} & \sqrt{\mathbb{E}[\|\bar{\mathbf{w}}_c^{(t+1)} - \bar{\mathbf{w}}^{(t+1)}\|^2]} \leq (1 + \eta_k \beta) \sqrt{\mathbb{E}[\|\bar{\mathbf{w}}_c^{(t)} - \bar{\mathbf{w}}^{(t)}\|^2]} + \eta_k \beta \sum_{d=1}^N \varrho_d \sqrt{\mathbb{E}[\|\bar{\mathbf{w}}_d^{(t)} - \bar{\mathbf{w}}^{(t)}\|^2]} \\ & + \eta_k \beta \epsilon_{c,k} + \eta_k \beta \epsilon_k + \eta_k (2\sigma + \zeta) + \sqrt{M \sum_{d=1}^N \varrho_d^2 \Theta_d^{(t+1)} \left(p_d \bar{\sigma}_{Loc}^2 + (1 - p_d) \sigma_{Loc}^2 \sum_{j \in \mathcal{S}_d} \rho_{j,d}^2 \right)} \\ & + \Theta_c^{(t+1)} \sqrt{M \left(p_c \bar{\sigma}_{Loc}^2 + (1 - p_c) \sigma_{Loc}^2 \sum_{j \in \mathcal{S}_c} \rho_{j,c}^2 \right)}. \end{aligned} \quad (86)$$

PROOF. First, note that if $\Theta_c^{(t+1)} = 1$, we have $\mathbf{e}_i^{(t+1)} = 0$. Consider $\Theta_c^{(t+1)} = 0$, to bound $\sqrt{\mathbb{E}[\|\mathbf{e}_i^{(t+1)}\|^2]}$, we first use the definition of $\mathbf{w}_i^{(t)}$ given in (13) and $\bar{\mathbf{w}}_c^{(t)}$ in (9) to get

$$\begin{aligned} \mathbf{w}_i^{(t+1)} - \bar{\mathbf{w}}_c^{(t+1)} &= [\mathbf{w}_i^{(t)} - \bar{\mathbf{w}}_c^{(t)}] - \eta_k \mathbf{n}_i^{(t)} + \eta_k \sum_{j \in \mathcal{S}_c} \rho_{j,c} \mathbf{n}_j^{(t)} \\ &- \eta_k \left[\nabla F_i(\mathbf{w}_i^{(t)}) - \nabla F_i(\bar{\mathbf{w}}_c^{(t)}) \right] + \eta_k \sum_{j \in \mathcal{S}_c} \rho_{j,c} \left[\nabla F_j(\mathbf{w}_j^{(t)}) - \nabla F_j(\bar{\mathbf{w}}_c^{(t)}) \right] \\ &- \eta_k \left[\nabla F_i(\bar{\mathbf{w}}_c^{(t)}) - \nabla \bar{F}_c(\bar{\mathbf{w}}_c^{(t)}) \right]. \end{aligned} \quad (87)$$

Taking the norm-2 from the both hand sides of the above equality gives us

$$\begin{aligned} \|\mathbf{e}_i^{(t+1)}\| &\leq \|\mathbf{w}_i^{(t)} - \bar{\mathbf{w}}_c^{(t)}\| + \eta_k \|\nabla F_i(\mathbf{w}_i^{(t)}) - \nabla F_i(\bar{\mathbf{w}}_c^{(t)})\| + \eta_k \|\mathbf{n}_i^{(t)}\| + \eta_k \left\| \sum_{j \in \mathcal{S}_c} \rho_{j,c} \mathbf{n}_j^{(t)} \right\| \\ &+ \eta_k \sum_{j \in \mathcal{S}_c} \rho_{j,c} \|\nabla F_j(\mathbf{w}_j^{(t)}) - \nabla F_j(\bar{\mathbf{w}}_c^{(t)})\| + \eta_k \|\nabla F_i(\bar{\mathbf{w}}_c^{(t)}) - \nabla \bar{F}_c(\bar{\mathbf{w}}_c^{(t)})\|. \end{aligned} \quad (88)$$

Using β -smoothness of $F_i(\cdot)$, $\forall i$, Assumption 2 and Jensen's inequality, we further bound the right hand side of (88) as

$$\|\mathbf{e}_i^{(t+1)}\| \leq (1 + \eta_k \beta) \|\mathbf{e}_i^{(t)}\| + \eta_k \beta \sum_{j \in \mathcal{S}_c} \rho_{j,c} \|\mathbf{e}_j^{(t)}\| + \eta_k \|\mathbf{n}_i^{(t)}\| + \eta_k \sum_{j \in \mathcal{S}_c} \rho_{j,c} \|\mathbf{n}_j^{(t)}\| + \eta_k \zeta_c. \quad (89)$$

Taking square and expectation of both hand sides of the above inequality and using Fact 1 (See Page 22) gives us

$$\sqrt{\mathbb{E}[\|\mathbf{e}_i^{(t+1)}\|^2]} \leq (1 + \eta_k \beta) \sqrt{\mathbb{E}[\|\mathbf{e}_i^{(t)}\|^2]} + \eta_k \beta \sum_{j \in \mathcal{S}_c} \rho_{j,c} \sqrt{\mathbb{E}[\|\mathbf{e}_j^{(t)}\|^2]} + \eta_k (2\sigma + \zeta_c). \quad (90)$$

Next, we establish an upper bound on $\sqrt{\mathbb{E}[\|\bar{\mathbf{w}}_c^{(t)} - \bar{\mathbf{w}}^{(t)}\|^2]}$. To determine the bound, we first express $\bar{\mathbf{w}}_c^{(t+1)}$ as

$$\bar{\mathbf{w}}_c^{(t+1)} = \bar{\mathbf{w}}_c^{(t)} - \eta_k \sum_{j \in \mathcal{S}_c} \rho_{j,c} \nabla F_j(\mathbf{w}_j^{(t)}) - \eta_k \sum_{j \in \mathcal{S}_c} \rho_{j,c} \mathbf{n}_j^{(t)} + \Theta_c^{(t+1)} \bar{\mathbf{n}}_{c,Loc}^{(t+1)}. \quad (91)$$

Also, $\bar{\mathbf{w}}^{(t+1)}$ can be written as

$$\bar{\mathbf{w}}^{(t+1)} = \bar{\mathbf{w}}^{(t)} - \eta_k \sum_{d=1}^N \varrho_d \sum_{j \in \mathcal{S}_d} \rho_{j,d} \nabla F_j(\mathbf{w}_j^{(t)}) - \eta_k \sum_{d=1}^N \varrho_d \sum_{j \in \mathcal{S}_d} \rho_{j,d} \mathbf{n}_j^{(t)} + \sum_{c=1}^N \varrho_c \Theta_c^{(t+1)} \bar{\mathbf{n}}_{c,Loc}^{(t+1)}. \quad (92)$$

Subtracting (91) from (92) and performing some algebraic manipulations gives us

$$\begin{aligned} \bar{\mathbf{w}}_c^{(t+1)} - \bar{\mathbf{w}}^{(t+1)} &= \bar{\mathbf{w}}_c^{(t)} - \bar{\mathbf{w}}^{(t)} - \eta_k \left[\nabla \bar{F}_c(\bar{\mathbf{w}}_c^{(t)}) - \nabla \bar{F}_c(\bar{\mathbf{w}}^{(t)}) \right] \\ &\quad - \eta_k \sum_{j \in \mathcal{S}_c} \rho_{j,c} \mathbf{n}_j^{(t)} + \eta_k \sum_{d=1}^N \varrho_d \sum_{j \in \mathcal{S}_d} \rho_{j,d} \mathbf{n}_j^{(t)} - \sum_{d=1}^N \varrho_d \Theta_d^{(t+1)} \bar{\mathbf{n}}_{d,Loc}^{(t+1)} + \Theta_c^{(t+1)} \bar{\mathbf{n}}_{c,Loc}^{(t+1)} \\ &\quad - \eta_k \sum_{j \in \mathcal{S}_c} \rho_{j,c} \left[\nabla F_j(\mathbf{w}_j^{(t)}) - \nabla F_j(\bar{\mathbf{w}}_c^{(t)}) \right] + \eta_k \sum_{d=1}^N \varrho_d \sum_{j \in \mathcal{S}_d} \rho_{j,d} \left[\nabla F_j(\mathbf{w}_j^{(t)}) - \nabla F_j(\bar{\mathbf{w}}_d^{(t)}) \right] \\ &\quad + \eta_k \sum_{d=1}^N \varrho_d \left[\nabla \bar{F}_d(\bar{\mathbf{w}}_d^{(t)}) - \nabla \bar{F}_d(\bar{\mathbf{w}}^{(t)}) \right] - \eta_k \left[\nabla \bar{F}_c(\bar{\mathbf{w}}^{(t)}) - \nabla F(\bar{\mathbf{w}}^{(t)}) \right]. \end{aligned} \quad (93)$$

Taking the norm-2 of both hand sides of the above equality along with applying the triangle inequality results in

$$\begin{aligned} \|\bar{\mathbf{w}}_c^{(t+1)} - \bar{\mathbf{w}}^{(t+1)}\| &\leq \|\bar{\mathbf{w}}_c^{(t)} - \bar{\mathbf{w}}^{(t)}\| + \eta_t \|\nabla \bar{F}_c(\bar{\mathbf{w}}_c^{(t)}) - \nabla \bar{F}_c(\bar{\mathbf{w}}^{(t)})\| \\ &\quad + \eta_k \left\| \sum_{j \in \mathcal{S}_c} \rho_{j,c} \mathbf{n}_j^{(t)} \right\| + \eta_k \left\| \sum_{d=1}^N \varrho_d \sum_{j \in \mathcal{S}_d} \rho_{j,d} \mathbf{n}_j^{(t)} \right\| + \left\| \sum_{d=1}^N \varrho_d \Theta_d^{(t+1)} \bar{\mathbf{n}}_{d,Loc}^{(t+1)} \right\| + \Theta_c^{(t+1)} \|\bar{\mathbf{n}}_{c,Loc}^{(t+1)}\| \\ &\quad + \eta_k \sum_{j \in \mathcal{S}_c} \rho_{j,c} \|\nabla F_j(\mathbf{w}_j^{(t)}) - \nabla F_j(\bar{\mathbf{w}}_c^{(t)})\| + \eta_k \sum_{d=1}^N \varrho_d \sum_{j \in \mathcal{S}_d} \rho_{j,d} \|\nabla F_j(\mathbf{w}_j^{(t)}) - \nabla F_j(\bar{\mathbf{w}}_d^{(t)})\| \\ &\quad + \eta_k \sum_{d=1}^N \varrho_d \|\nabla \bar{F}_d(\bar{\mathbf{w}}_d^{(t)}) - \nabla \bar{F}_d(\bar{\mathbf{w}}^{(t)})\| + \eta_k \|\nabla \bar{F}_c(\bar{\mathbf{w}}^{(t)}) - \nabla F(\bar{\mathbf{w}}^{(t)})\|. \end{aligned} \quad (94)$$

Using Assumption 2 and Jensen's inequality, we further bound the right hand side of (94) to get

$$\begin{aligned} \|\bar{\mathbf{w}}_c^{(t+1)} - \bar{\mathbf{w}}^{(t+1)}\| &\leq (1 + \eta_k \beta) \|\bar{\mathbf{w}}_c^{(t)} - \bar{\mathbf{w}}^{(t)}\| + \eta_k \beta \sum_{d=1}^N \varrho_d \|\bar{\mathbf{w}}_d^{(t)} - \bar{\mathbf{w}}^{(t)}\| + \eta_k \left\| \sum_{j \in \mathcal{S}_c} \rho_{j,c} \mathbf{n}_j^{(t)} \right\| \\ &\quad + \eta_k \left\| \sum_{d=1}^N \varrho_d \sum_{j \in \mathcal{S}_d} \rho_{j,d} \mathbf{n}_j^{(t)} \right\| + \left\| \sum_{d=1}^N \varrho_d \Theta_d^{(t+1)} \bar{\mathbf{n}}_{d,Loc}^{(t+1)} \right\| + \Theta_c^{(t+1)} \|\bar{\mathbf{n}}_{c,Loc}^{(t+1)}\| \\ &\quad + \eta_k \beta \sum_{j \in \mathcal{S}_c} \rho_{j,c} \|\mathbf{e}_j^{(t)}\| + \eta_k \beta \sum_{d=1}^N \varrho_d \sum_{j \in \mathcal{S}_d} \rho_{j,d} \|\mathbf{e}_j^{(t)}\| + \eta_k \zeta. \end{aligned} \quad (95)$$

To obtain the one-step behavior of $\sqrt{\mathbb{E}[\|\bar{\mathbf{w}}_c^{(t+1)} - \bar{\mathbf{w}}^{(t+1)}\|^2]}$, we take square and expectation from both hand sides of the above inequality and using Fact 1 (See Page 22) to get

$$\begin{aligned} \sqrt{\mathbb{E}[\|\bar{\mathbf{w}}_c^{(t+1)} - \bar{\mathbf{w}}^{(t+1)}\|^2]} &\leq (1 + \eta_k \beta) \sqrt{\mathbb{E}[\|\bar{\mathbf{w}}_c^{(t)} - \bar{\mathbf{w}}^{(t)}\|^2]} + \eta_k \beta \sum_{d=1}^N \varrho_d \sqrt{\mathbb{E}[\|\bar{\mathbf{w}}_d^{(t)} - \bar{\mathbf{w}}^{(t)}\|^2]} \\ &\quad + \eta_k \beta \epsilon_{c,k} + \eta_k \beta \epsilon_k + \eta_k (2\sigma + \zeta) + \sqrt{\mathbb{E} \left\| \sum_{d=1}^N \varrho_d \Theta_d^{(t+1)} \bar{\mathbf{n}}_{d,Loc}^{(t+1)} \right\|^2} + \Theta_c^{(t+1)} \sqrt{\mathbb{E} \|\bar{\mathbf{n}}_{c,Loc}^{(t+1)}\|^2}. \end{aligned} \quad (96)$$

To bound $\sqrt{\mathbb{E} \left\| \sum_{d=1}^N \varrho_d \Theta_d^{(t)} \bar{\mathbf{n}}_{d,Loc}^{(t+1)} \right\|^2}$ and $\sqrt{\mathbb{E} \|\bar{\mathbf{n}}_{c,Loc}^{(t+1)}\|^2}$ above, we first apply the law of total expectation to obtain

$$\begin{aligned} &\mathbb{E}[\|\bar{\mathbf{n}}_{c,Loc}^{(t+1)}\|^2] \\ &= p_c \cdot \mathbb{E} \left[\left\| \tilde{\bar{\mathbf{n}}}_{c,Loc}^{(t+1)} \right\|^2 \middle| \tilde{\bar{\mathbf{n}}}_{c,Loc}^{(t+1)} \sim \mathcal{N}(0, \bar{\sigma}_{Loc}^2) \right] + (1 - p_c) \cdot \mathbb{E} \left[\left\| \sum_{j \in \mathcal{S}_c} \rho_{j,c} \mathbf{n}_{j,Loc}^{(t+1)} \right\|^2 \middle| \mathbf{n}_{j,Loc}^{(t+1)} \sim \mathcal{N}(0, \sigma_{Loc}^2) \right] \end{aligned}$$

$$\stackrel{(i)}{=} p_c \underbrace{\mathbb{E} \left[\left\| \bar{\mathbf{n}}_{c,Loc}^{(t+1)} \right\|^2 \middle| \bar{\mathbf{n}}_{c,Loc}^{(t+1)} \sim \mathcal{N}(0, \bar{\sigma}_{Loc}^2) \right]}_{(a_1)} + (1-p_c) \sum_{j \in \mathcal{S}_c} \rho_{j,c}^2 \underbrace{\mathbb{E} \left[\left\| \mathbf{n}_{j,Loc}^{(t+1)} \right\|^2 \middle| \mathbf{n}_{j,Loc}^{(t+1)} \sim \mathcal{N}(0, \sigma_{Loc}^2) \right]}_{(a_2)}. \quad (97)$$

where (i) comes from the fact that $\mathbf{n}_{j,Loc}^{(t)}$ are i.i.d. random variables for $j \in \mathcal{S}_c$. To bound (a₁) in the above inequality, we show that

$$\mathbb{E} \left[\left\| \bar{\mathbf{n}}_{c,Loc}^{(t+1)} \right\|^2 \middle| \bar{\mathbf{n}}_{c,Loc}^{(t+1)} \sim \mathcal{N}(0, \bar{\sigma}_{Loc}^2) \right] = \mathbb{E} \left[\sum_{n=0}^{M-1} (\bar{n}_{\{c,n\},Loc}^{(t+1)})^2 \right] = \sum_{n=0}^{M-1} \mathbb{E} \left[(\bar{n}_{\{c,n\},Loc}^{(t+1)})^2 \right] = M \bar{\sigma}_{Loc}^2, \quad (98)$$

where $\bar{\mathbf{n}}_{c,Loc}^{(t+1)} = (\bar{n}_{\{c,0\},Loc}^{(t+1)}, \bar{n}_{\{c,1\},Loc}^{(t+1)}, \dots, \bar{n}_{\{c,M-1\},Loc}^{(t+1)})$. Similarly, to bound (a₂), we show that

$$\mathbb{E} \left[\left\| \mathbf{n}_{j,Loc}^{(t+1)} \right\|^2 \middle| \mathbf{n}_{j,Loc}^{(t+1)} \sim \mathcal{N}(0, \sigma_{Loc}^2) \right] = \mathbb{E} \left[\sum_{n=0}^{M-1} (n_{\{j,n\},Loc}^{(t+1)})^2 \right] = \sum_{n=0}^{M-1} \mathbb{E} \left[(n_{\{j,n\},Loc}^{(t+1)})^2 \right] = M \sigma_{Loc}^2, \quad (99)$$

where $\mathbf{n}_{j,Loc}^{(t+1)} = (n_{\{j,0\},Loc}^{(t+1)}, n_{\{j,1\},Loc}^{(t+1)}, \dots, n_{\{j,M-1\},Loc}^{(t+1)})$. Replacing (48) and (49) into (97) gives us

$$\mathbb{E} [\|\bar{\mathbf{n}}_{c,Loc}^{(t+1)}\|^2] = M \left(p_c \bar{\sigma}_{Loc}^2 + (1-p_c) \sigma_{Loc}^2 \sum_{j \in \mathcal{S}_c} \rho_{j,c}^2 \right). \quad (100)$$

Similarly, we can also use (98), (99) and the fact that $\bar{\mathbf{n}}_{c,Loc}^{(t)}$ are i.i.d. random variables for $c = 1, 2, \dots, N$ to obtain

$$\begin{aligned} \mathbb{E} \left[\left\| \sum_{d=1}^N \varrho_d \Theta_d^{(t+1)} \bar{\mathbf{n}}_{d,Loc}^{(t+1)} \right\|^2 \right] &= \sum_{d=1}^N \varrho_d^2 \Theta_d^{(t+1)} \mathbb{E} [\|\bar{\mathbf{n}}_{d,Loc}^{(t+1)}\|^2] \\ &= M \sum_{d=1}^N \varrho_d^2 \Theta_d^{(t+1)} \left(p_d \bar{\sigma}_{Loc}^2 + (1-p_d) \sigma_{Loc}^2 \sum_{j \in \mathcal{S}_d} \rho_{j,d}^2 \right), \end{aligned} \quad (101)$$

Replacing (100) and (101) into (96) yields

$$\begin{aligned} \sqrt{\mathbb{E} [\|\bar{\mathbf{w}}_c^{(t+1)} - \bar{\mathbf{w}}^{(t+1)}\|^2]} &\leq (1 + \eta_k \beta) \sqrt{\mathbb{E} [\|\bar{\mathbf{w}}_c^{(t)} - \bar{\mathbf{w}}^{(t)}\|^2]} + \eta_k \beta \sum_{d=1}^N \varrho_d \sqrt{\mathbb{E} [\|\bar{\mathbf{w}}_d^{(t)} - \bar{\mathbf{w}}^{(t)}\|^2]} \\ &+ \eta_k \beta \epsilon_{c,k} + \eta_k \beta \epsilon_k + \eta_k (2\sigma + \zeta) + \sqrt{M \sum_{d=1}^N \varrho_d^2 \Theta_d^{(t+1)} \left(p_d \bar{\sigma}_{Loc}^2 + (1-p_d) \sigma_{Loc}^2 \sum_{j \in \mathcal{S}_d} \rho_{j,d}^2 \right)} \\ &+ \Theta_c^{(t+1)} \sqrt{M \left(p_c \bar{\sigma}_{Loc}^2 + (1-p_c) \sigma_{Loc}^2 \sum_{j \in \mathcal{S}_c} \rho_{j,c}^2 \right)}. \end{aligned} \quad (102)$$

□

LEMMA C.3. Under Assumption 2, we have

$$\begin{aligned} & - \eta_k \sum_{\ell=t_k}^{t_{k+1}-1} \left[\nabla F(\bar{\mathbf{w}}^{(t_k)})^\top \sum_{c=1}^N \varrho_c \sum_{j \in \mathcal{S}_c} \rho_{j,c} \nabla F_j(\mathbf{w}_j^{(\ell)}) \right] \leq -\frac{\eta_k \tau}{2} \left\| \nabla F(\bar{\mathbf{w}}^{(t_k)}) \right\|^2 \\ & - \frac{\eta_k}{2} \sum_{\ell=t_k}^{t_{k+1}-1} \left\| \sum_{c=1}^N \varrho_c \sum_{j \in \mathcal{S}_c} \rho_{j,c} \nabla F_j(\mathbf{w}_j^{(\ell)}) \right\|^2 + \frac{\eta_k \beta^2}{2} \sum_{\ell=t_k}^{t_{k+1}-1} \sum_{c=1}^N \varrho_c \sum_{j \in \mathcal{S}_c} \rho_{j,c} \left\| \bar{\mathbf{w}}^{(\ell)} - \mathbf{w}_j^{(\ell)} \right\|^2 + \frac{\eta_k^3 \beta^2 \tau^2 G^2}{2}. \end{aligned}$$

PROOF. Since $-2\mathbf{a}^\top \mathbf{b} = -\|\mathbf{a}\|^2 - \|\mathbf{b}\|^2 + \|\mathbf{a} - \mathbf{b}\|^2$ holds for any two vectors \mathbf{a} and \mathbf{b} with real elements, we have

$$\begin{aligned} & - \eta_k \sum_{\ell=t_k}^{t_{k+1}-1} \left[\nabla F(\bar{\mathbf{w}}^{(t_k)})^\top \sum_{c=1}^N \varrho_c \sum_{j \in \mathcal{S}_c} \rho_{j,c} \nabla F_j(\mathbf{w}_j^{(\ell)}) \right] \\ & = \frac{\eta_k}{2} \sum_{\ell=t_k}^{t_{k+1}-1} \left[-\left\| \nabla F(\bar{\mathbf{w}}^{(t_k)}) \right\|^2 - \left\| \sum_{c=1}^N \varrho_c \sum_{j \in \mathcal{S}_c} \rho_{j,c} \nabla F_j(\mathbf{w}_j^{(\ell)}) \right\|^2 \right] \end{aligned}$$

$$+ \underbrace{\left\| \nabla F(\bar{\mathbf{w}}^{(t_k)}) - \sum_{c=1}^N \varrho_c \sum_{j \in \mathcal{S}_c} \rho_{j,c} \nabla F_j(\mathbf{w}_j^{(\ell)}) \right\|^2}_{(a)}. \quad (103)$$

Applying Assumption 2, we further bound (a) above as

$$\begin{aligned} & \left\| \nabla F(\bar{\mathbf{w}}^{(t_k)}) - \sum_{c=1}^N \varrho_c \sum_{j \in \mathcal{S}_c} \rho_{j,c} \nabla F_j(\mathbf{w}_j^{(\ell)}) \right\|^2 \\ & \stackrel{(i)}{\leq} \sum_{c=1}^N \varrho_c \sum_{j \in \mathcal{S}_c} \rho_{j,c} \left\| \nabla F_j(\bar{\mathbf{w}}^{(t_k)}) - \nabla F_j(\mathbf{w}_j^{(\ell)}) \right\|^2 \\ & \stackrel{(ii)}{\leq} \underbrace{\beta^2 \sum_{c=1}^N \varrho_c \sum_{j \in \mathcal{S}_c} \rho_{j,c} \left\| \bar{\mathbf{w}}^{(t_k)} - \mathbf{w}_j^{(\ell)} \right\|^2}_{(b)}, \end{aligned} \quad (104)$$

where (i) involves the application of Jensen's inequality, and (ii) utilizes the β -smoothness of $F_i(\cdot)$ as described in Assumption 2. We further upper bound term (b) as follows:

$$\begin{aligned} & \sum_{c=1}^N \varrho_c \sum_{j \in \mathcal{S}_c} \rho_{j,c} \left\| \bar{\mathbf{w}}^{(t_k)} - \mathbf{w}_j^{(\ell)} \right\|^2 = \sum_{c=1}^N \varrho_c \sum_{j \in \mathcal{S}_c} \rho_{j,c} \left\| \bar{\mathbf{w}}^{(t_k)} - \bar{\mathbf{w}}^{(\ell)} + \bar{\mathbf{w}}^{(\ell)} - \mathbf{w}_j^{(\ell)} \right\|^2 \\ & \leq \left\| \bar{\mathbf{w}}^{(t_k)} - \bar{\mathbf{w}}^{(\ell)} \right\|^2 + \sum_{c=1}^N \varrho_c \sum_{j \in \mathcal{S}_c} \rho_{j,c} \left\| \bar{\mathbf{w}}^{(\ell)} - \mathbf{w}_j^{(\ell)} \right\|^2, \end{aligned} \quad (105)$$

where, in the last step, we used the fact that $\sum_{c=1}^N \varrho_c \sum_{j \in \mathcal{S}_c} \rho_{j,c} (\bar{\mathbf{w}}^{(t_k)} - \bar{\mathbf{w}}^{(\ell)})^\top (\bar{\mathbf{w}}^{(\ell)} - \mathbf{w}_j^{(\ell)}) = 0$. Upper bound (103) with (104) and (105) yields

$$\begin{aligned} & -\eta_k \sum_{\ell=t_k}^{t_{k+1}-1} \left[\nabla F(\bar{\mathbf{w}}^{(t_k)})^\top \sum_{c=1}^N \varrho_c \sum_{j \in \mathcal{S}_c} \rho_{j,c} \nabla F_j(\mathbf{w}_j^{(\ell)}) \right] \leq -\tau \mu \eta_k (F(\bar{\mathbf{w}}^{(t_k)}) - F(\mathbf{w}^*)) \\ & - \frac{\eta_k}{2} \sum_{\ell=t_k}^{t_{k+1}-1} \left\| \sum_{c=1}^N \varrho_c \sum_{j \in \mathcal{S}_c} \rho_{j,c} \nabla F_j(\mathbf{w}_j^{(\ell)}) \right\|^2 + \underbrace{\frac{\eta_k \beta^2}{2} \sum_{\ell=t_k}^{t_{k+1}-1} \left\| \bar{\mathbf{w}}^{(t_k)} - \bar{\mathbf{w}}^{(\ell)} \right\|^2}_{(c)} \\ & + \frac{\eta_k \beta^2}{2} \sum_{\ell=t_k}^{t_{k+1}-1} \sum_{c=1}^N \varrho_c \sum_{j \in \mathcal{S}_c} \rho_{j,c} \left\| \bar{\mathbf{w}}^{(\ell)} - \mathbf{w}_j^{(\ell)} \right\|^2. \end{aligned} \quad (106)$$

We can further upper bound (c) as follows:

$$\sum_{\ell=t_k}^{t_{k+1}-1} \left\| \bar{\mathbf{w}}^{(t_k)} - \bar{\mathbf{w}}^{(\ell)} \right\|^2 \leq \eta_k^2 \tau \left\| \sum_{m=t_k}^{t_{k+1}-1} \sum_{c=1}^N \varrho_c \sum_{j \in \mathcal{S}_c} \rho_{j,c} \widehat{\mathbf{g}}_j^{(m)} \right\|^2 \stackrel{(c-i)}{\leq} \eta_k^2 \tau^2 G^2, \quad (107)$$

where last step results from the clipping operation. Replacing the result of (107) into (106) concludes the proof. \square

FACT 1. Consider n random real-valued vectors $\mathbf{x}_1, \dots, \mathbf{x}_n \in \mathbb{R}^m$, the following inequality holds:

$$\sqrt{\mathbb{E} \left[\left\| \sum_{i=1}^n \mathbf{x}_i \right\|^2 \right]} \leq \sum_{i=1}^n \sqrt{\mathbb{E} [\|\mathbf{x}_i\|^2]}. \quad (108)$$

PROOF. Note that

$$\sqrt{\mathbb{E} \left[\left\| \sum_{i=1}^n \mathbf{x}_i \right\|^2 \right]} = \sqrt{\sum_{i,j=1}^n \mathbb{E} [\mathbf{x}_i^\top \mathbf{x}_j]} \stackrel{(a)}{\leq} \sum_{i,j=1}^n \sqrt{\mathbb{E} [\|\mathbf{x}_i\|^2] \mathbb{E} [\|\mathbf{x}_j\|^2]} = \sum_{i=1}^n \sqrt{\mathbb{E} [\|\mathbf{x}_i\|^2]}, \quad (109)$$

where (a) follows from Holder's inequality, $\mathbb{E} [|\mathbf{X}\mathbf{Y}|] \leq \sqrt{\mathbb{E} [|\mathbf{X}|^2] \mathbb{E} [|\mathbf{Y}|^2]}$. \square

FACT 2. Let $a \geq 0$, $b \geq 0$ and $n \geq 1$ (or $n \geq 0$ if n integer). Then, it follows $a^n - b^n \leq (a - b)na^{n-1}$.

PROOF. Let $\phi(x) \triangleq a^n - (a + x)^n$. Since $\phi(x)$ is a concave function of $x \geq -a$, it follows that $a^n - b^n = \phi(b - a) \leq \phi(0) + \phi'(0)(b - a) = (a - b)na^{n-1}$. \square

D ENERGY AND DELAY CONSUMPTION MODELS

The energy and delay model for our system accounts for various factors including model size M , quantization level Q , individual device transmit power p_j , and transmission rates $R_j^{(t)}$, as outlined in [11]. Transmission rates are influenced by the device's power, channel conditions represented by $h_j^{(t)}$, and the system's noise power, denoted as N_0W for bandwidth W .

Local energy consumption at an edge server, $E_{c,Loc} = \sum_{j \in S_c^k} p_j \cdot M \cdot Q / R_j^{(t)}$, is computed by aggregating the energy from devices in the cluster S_c^k . Global energy consumption, $E_{GlobAgg} = \sum_{c=1}^N \bar{p}_{n_c} \cdot M \cdot Q / \bar{R}_{n_c}^{(t)}$, sums the energy for communications between all edge servers and the central server, taking into account each server's transmit power \bar{p}_{n_c} and transmission rate $\bar{R}_{n_c}^{(t)}$.

Regarding delays, $\Delta_{c,Loc}$ quantifies the total transmission time for all selected devices in cluster c to send their model updates, expressed as $\Delta_{c,Loc} = \sum_{j \in S_c^k} M \cdot Q / R_j^{(t)}$. Meanwhile, the global aggregation delay, Δ_{Glob} , sums up the communication times between all edge servers and the main server, given by $\Delta_{Glob} = \sum_{c=1}^N M \cdot Q / \bar{R}_{n_c}^{(t)}$ ⁴.

Wireless communications between devices and the edge employ a standard transmit power of $p_i = 24$ dBm per device, with a bandwidth of $W = 1$ MHz and a noise spectral density of $N_0 = -173$ dBm/Hz. Following the model from [22], pathloss and fading are calculated using $h_i^{(t)} = \sqrt{\beta_i^{(t)}} u_i^{(t)}$, where $\beta_i^{(t)} = \beta_0 - 10\hat{\alpha} \log_{10}(d_i^{(t)}/d_0)$, $\beta_0 = -30$ dB, and $\hat{\alpha} = 3.75$. Rayleigh fading is modeled with $u_i^{(t)} \sim CN(0, 1)$, and $d_i^{(t)}$ is the distance to the edge server. For wired communications from edge to cloud, the transmit power is set at $\bar{p}_{n_c} = 38$ dBm with a data rate of $\bar{R}_{n_c}^{(t)} = 100$ Mbps.

⁴In the optimization framework for communication systems, while the most intuitive measure of delay is often to consider the maximum transmission time—since it represents the actual bottleneck time required for all devices to complete their transmissions—here we choose to use the total sum of transmission times instead. This approach provides several advantages. By considering the cumulative delay, the framework more accurately reflects the resource utilization across the network. This comprehensive view allows for more effective optimization of network resources, as it enables the identification of efficiencies and redundancies in the data transmission process. Utilizing the total delay helps in balancing the load more evenly among devices and can encourage solutions that not only focus on the slowest link but optimize the overall system performance.

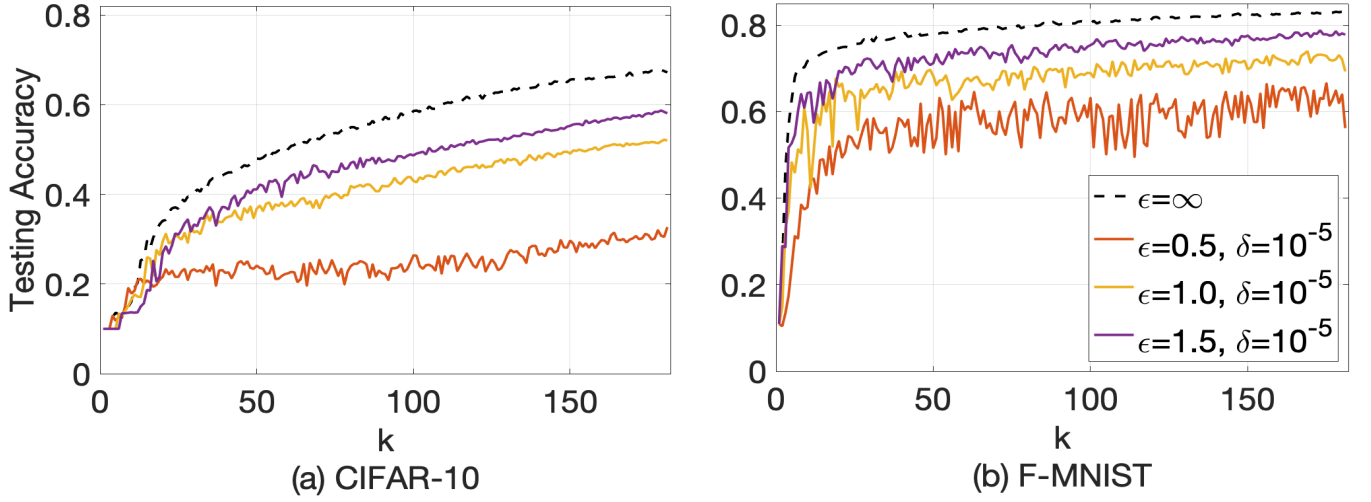


FIGURE 9: Impact of varying privacy budgets (ϵ) per entity on the training performance of H^2FDP . It illustrates that the testing accuracy for both datasets improves as the allocated privacy budget ϵ increases.

E ADDITIONAL EXPERIMENTAL RESULTS

This section presents the plots from complimentary experiments mentioned in Sec. 6. Fig 9 presents the training performance of H^2FDP for varying privacy protection ϵ , with $p_c = 0.5$. When the privacy budget allocated to each entity decreases – for instance, moving from $\epsilon = 1$ down to $\epsilon = 0.5$ – a corresponding decline in H^2FDP 's accuracy is observed. This manifests as approximately a 20% and 13% dip in testing accuracy by $k = 200$ for CIFAR-10 and F-MNIST respectively. A consequential side effect of this lower privacy budget is the enhanced volatility detected in the accuracy curve, especially when $\epsilon = 0.5$. Conversely, when the privacy budget per entity is escalated (in this case, moving from $\epsilon = 1$ to $\epsilon = 1.5$), the H^2FDP algorithm displays a surge in performance. This improvement equates to a rise in accuracy by about 6.1% for CIFAR-10 and 8.5% for F-MNIST. In addition, a higher privacy budget appears to stabilize the volatility in the accuracy curve, leading to a more steady performance when compared to the setting with a privacy budget of $\epsilon = 1$. Naturally, our benchmark model, which does not incorporate any privacy guarantees, showcases optimal performance and stability. This stark contrast underscores the inherent trade-off that exists when incorporating privacy provisions into FL models.

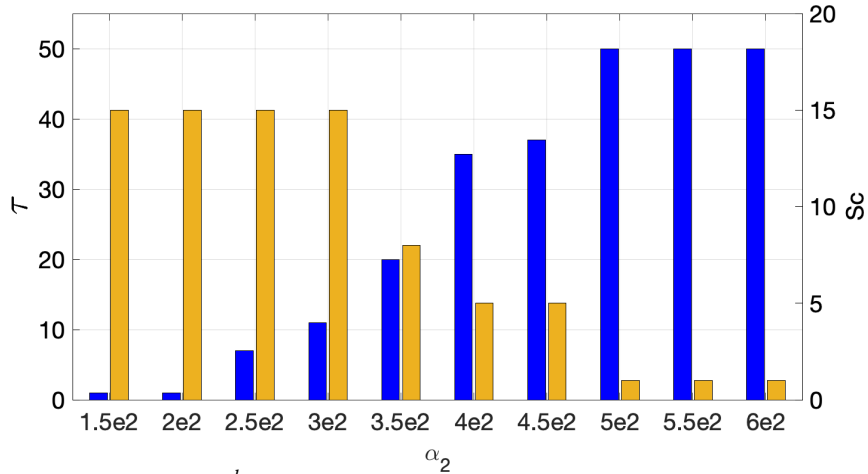


FIGURE 10: Average values of τ_k and s_c^k chosen by Algorithm 1 across various configurations of coefficient α_2 .

Fig. 10 illustrates the impact of adjusting the optimization weight α_2 within the control algorithm \mathcal{P} . The influence of α_1 and α_2 on the decision variable is similar. Specifically, an increase in α_2 , which emphasizes communication energy, leads to (i) longer training intervals τ , due to reduced frequency of global aggregations that minimize communication demands, and (ii) a smaller number s_c of devices participating in training, effectively lowering communication overhead.

Algorithm 2: Overall H²FDP procedure.

Input: Length of training T , number of global aggregations K_g , length of local aggregation periods m_k , length of local model training intervals τ_k , learning rates η_k , minibatch sizes $|\xi_i^{(t)}|$

Output: Final global model $\bar{\mathbf{w}}(T)$

```

1 Initialize  $\bar{\mathbf{w}}^{(0)}$  and broadcast it across edge servers and devices, resulting in  $\bar{\mathbf{w}}_c^{(0)} = \bar{\mathbf{w}}^{(0)}$ ,  $\forall c$  and  $\mathbf{w}_i^{(0)} = \bar{\mathbf{w}}^{(0)}$ ,  $i \in \mathcal{I}$ .
2 for  $k = 0 : K_g - 1$  do
3   for  $t = t_k + 1 : t_{k+1}$  do
4     for  $c = 1 : N$  do // Procedure at each subnet  $\mathcal{S}_c$ 
5       Local SGD update with:  $\bar{\mathbf{w}}_i^{(t)} = \mathbf{w}_i^{(t-1)} - \eta_{t-1} \hat{\mathbf{g}}_i^{(t-1)}$ ;
6       if  $t \in \mathcal{T}_{k,c}^L$  then
7         if  $n_c \in \mathcal{N}_T$  then
8           Edge device  $i$  sends accumulated gradients  $\eta_k \sum_{\ell=t-m_k}^t \hat{\mathbf{g}}_i^{(\ell)}$  via uplink transmission;
9           Edge server  $n_c$  conducts local aggregation with:  $\bar{\mathbf{w}}_c^{(t)} = \bar{\mathbf{w}}_c^{(t-m_k)} - \eta_k \sum_{\ell=t-m_k}^t \sum_{j \in \mathcal{S}_c} \rho_{j,c} \hat{\mathbf{g}}_j^{(\ell)} + \bar{\mathbf{n}}_{c,Loc}^{(t)}$  and  $\mathbf{w}_i^{(t)} = \bar{\mathbf{w}}_c^{(t)}$ ;
10          else
11            Edge device  $i$  sends noisy accumulated gradients  $\eta_k \sum_{\ell=t-m_k}^t \hat{\mathbf{g}}_i^{(\ell)} + \mathbf{n}_{i,Loc}^{(t)}$  via uplink transmission;
12            Edge server conducts local aggregation with:  $\bar{\mathbf{w}}_c^{(t)} = \bar{\mathbf{w}}_c^{(t-m_k)} - \eta_k \sum_{\ell=t-m_k}^t \sum_{j \in \mathcal{S}_c} \rho_{j,c} \hat{\mathbf{g}}_j^{(\ell)} + \sum_{j \in \mathcal{S}_c} \rho_{j,c} \mathbf{n}_{j,Loc}^{(t)}$  and  $\mathbf{w}_i^{(t)} = \bar{\mathbf{w}}_c^{(t)}$ ;
13          else
14             $\mathbf{w}_i^{(t)} = \bar{\mathbf{w}}_i^{(t)}$ .
15      if  $t = t_{k+1}$  then
16        for  $c = 1 : N$  do // Procedure at each subnet  $\mathcal{S}_c$ 
17          if  $n_c \in \mathcal{N}_T$  then
18            Edge device  $i$  sends accumulated gradients  $\eta_k \sum_{\ell=t-m_k}^t \hat{\mathbf{g}}_i^{(\ell)}$  via uplink transmission;
19            Edge server  $n_c$  computes and sends  $\eta_k \sum_{\ell=t-m_k}^t \sum_{j \in \mathcal{S}_c} \rho_{j,c} \hat{\mathbf{g}}_j^{(\ell)} + \bar{\mathbf{n}}_{c,Glob}^{(t)}$  via uplink transmission;
20          else
21            Edge device  $i$  sends noisy accumulated gradients  $\eta_k \sum_{\ell=t-m_k}^t \hat{\mathbf{g}}_i^{(\ell)} + \mathbf{n}_{i,Glob}^{(t)}$  via uplink transmission;
22            Edge server computes and sends  $\eta_k \sum_{\ell=t-m_k}^t \sum_{j \in \mathcal{S}_c} \rho_{j,c} \hat{\mathbf{g}}_j^{(\ell)} + \sum_{j \in \mathcal{S}_c} \rho_{j,c} \mathbf{n}_{j,Glob}^{(t)}$  via uplink transmission;
23          Main server performs global aggregation via (14) and downlink broadcast;

```

F PSEUDOCODE H²FDP WITHOUT CONTROL

The full H²FDP procedure is summarized in Algorithm 2.